

SEGDAC: IMPROVING VISUAL REINFORCEMENT LEARNING BY EXTRACTING DYNAMIC OBJECT-CENTRIC REPRESENTATIONS FROM PRETRAINED VISION MODELS

Alexandre Brown

alexandre.brown@mila.quebec
Mila Quebec AI Institute
Université de Montréal

Glen Berseth

glen.berseth@mila.quebec
Mila Quebec AI Institute
Université de Montréal

ABSTRACT

Visual reinforcement learning (RL) is challenging due to the need to extract useful representations from high-dimensional inputs while learning effective control from sparse and noisy rewards. Although large perception models exist, integrating them effectively into RL for visual generalization and improved sample efficiency remains difficult. We propose **SegDAC**, a **Segmentation-Driven Actor-Critic** method. SegDAC uses Segment Anything (SAM) for object-centric decomposition and YOLO-World to ground the image segmentation process via text inputs. It includes a novel transformer-based architecture that supports a dynamic number of segments at each time step and effectively learns which segments to focus on using online RL, without using human labels. By evaluating SegDAC over a challenging visual generalization benchmark using Maniskill3, which covers diverse manipulation tasks under strong visual perturbations, we demonstrate that SegDAC achieves significantly better visual generalization, doubling prior performance on the hardest setting and matching or surpassing prior methods in sample efficiency across all evaluated tasks.

1 INTRODUCTION

Reinforcement learning (RL) from images is challenging because of the high dimensionality of visual inputs, their variability across environments and the limited robustness of policies under visual perturbations (Mnih et al., 2013; Pathak et al., 2017; Yarats et al., 2020; Lepert et al., 2024; Yuan et al., 2023; Lyu et al., 2024; Lepert et al., 2024). A natural idea is to leverage pre-trained vision models, but integrating them into online RL has proven to be challenging; one must choose the right layer to feed into the policy, manage inference costs during large-scale experience collection, and potentially adapt features that were not designed for RL in the first place. In parallel, many visual RL methods rely on data augmentation to improve robustness, while this can help, it adds complexity and does not address the core issue of learning meaningful general structure from images.

Images, like sentences, have an inherent structure. Words in a sentence carry meaning beyond individual characters, and similarly, objects in a scene provide more useful building blocks than raw pixels or patches (Chen et al., 2024; 2025; Locatello et al., 2020; Wang et al., 2023). Conventional pixel-based methods extract features from uniform grids, overlooking the object-level structure of the scene. By contrast, object-centric representations can capture entities and their relationships, offering a more abstract and semantically meaningful description of the environment. Prior segmentation-based RL approaches have explored this direction by decomposing an image into segments, meaning distinct parts of the image, but they often relied on fixed slots, precomputed masks, or strong supervision, which limited their flexibility and general applicability.

To overcome the above issues, we introduce **SegDAC** (**Segmentation-Driven Actor-Critic**), a simple yet powerful RL method that addresses these limitations. SegDAC leverages pretrained vision models to perform dynamic, text-grounded semantic segmentation at every frame, producing a variable

set of object-centric embeddings. These embeddings are processed by a transformer-based actor-critic architecture with carefully designed segment processing, analogous to how Vision Transformers (Dosovitskiy et al., 2021) adapt a standard transformer encoder for image patches. Our design specifies how to represent image segments as tokens, define queries and keys, and merge action information. This design enables the policy to adapt computation to the complexity of each scene, rather than relying on fixed representations. Unlike most visual RL methods (Yarats et al., 2020; 2021; Grooten et al., 2023; Almuzairee et al., 2024), SegDAC learns entirely in latent space, without human-labeled masks, auxiliary losses, or data augmentation, making it both easier to use and more extensible. Our main contributions are therefore: **Dynamic object-centric RL**: Transformer-based policies that can natively process a variable number of object-centric representations that are dynamically computed at each time step, allowing adaptive compute depending on scene complexity while avoiding per-task architectural tuning or image segments limit. **First successful use of text-grounded segmentation for online RL**: We provide an architecture (see fig. 2) that leverages text information to semantically ground the segmentation process more effectively and show its effectiveness in online RL. **Improved visual generalization and sample efficiency**: Prior visual RL methods have typically achieved either strong sample efficiency at the cost of poor visual generalization, or better generalization at the cost of slower learning. On ManiSkill3 (Tao et al., 2024) tasks with custom-designed benchmark featuring challenging out-of-distribution visual perturbations, SegDAC is the first to demonstrate strong performance in both dimensions, achieving up to 2x gains under the most challenging visual generalization setting while matching or exceeding the sample efficiency of state-of-the-art baselines.

2 RELATED WORK

We review prior work in model-free visual RL along three main themes: (1) learning directly from pixels, (2) leveraging pretrained models, and (3) segmentation/object-centric approaches. Tables 1 and 45 summarize how SegDAC compares.

RL from Images: Several model-free RL methods aimed to improve sample efficiency or robustness directly from pixels. SAC-AE (Yarats et al., 2020) used auxiliary reconstruction losses. RAD (Laskin et al., 2020), DrQ (Kostrikov et al., 2021), SODA (Hansen & Wang, 2021), SVEA (Hansen et al., 2021), DrQ-v2 (Yarats et al., 2021), and later methods such as MaDi (Grooten et al., 2023) and SADA (Almuzairee et al., 2024) improved generalization through data augmentation and training stabilizers. While effective, these approaches remained pixel-based. SegDAC avoids auxiliary losses and data augmentations entirely, showing that strong generalization can be achieved without techniques previously considered necessary. **Pretrained Vision Models in RL**: PIE-G (Yuan et al., 2022), SAM-G (Wang et al., 2023), and IWM (Garrido et al., 2024) all adapted ImageNet pretrained encoders for RL. PIE-G remained pixel-based. SAM-G, built on PIE-G, used offline SAM features with human labels, fixing object representations before training. IWM applied pretrained encoders in a world model framework. SegDAC differs by integrating pretrained segmentation and detection models directly in online RL, producing dynamic, text-grounded object embeddings without labels or offline datasets. **Segmentation for RL**: Segmentation has been used in RL either to train a segmentation model with RL signals (Melnik et al., 2021) or to guide policies using SAM (Kirillov et al., 2023). Saliency-based methods predicted pixels of interest but lacked semantic abstraction (Wu et al., 2021; Wang et al., 2021; Bertoin et al., 2023). SAM-G (Wang et al., 2023) relied on

Table 1: Comparison of segmentation-based visual RL methods.

Criterion	SAM-G	FTD	SegDAC (ours)
Needs Human Labels	✗ Yes	✓ No	✓ No
Leverages Pretrained Vision Models	✓ Yes	✓ Yes	✓ Yes
Leverages Text	✗ No	✗ No	✓ Yes
Representations / Frame	✗ Fixed objects	✗ Fixed N slots	✓ Dynamic
Representations Computation	✗ Offline (per-task)	✓ Online (per-step)	✓ Online (per-step)
Learns In Latent Space	✗ No (masked pixels)	✗ No (masked pixels)	✓ Yes (objects embeddings)
Needs Auxiliary Losses	✓ No	✗ Yes	✓ No
Needs Data Aug. (RL Training)	✗ Yes	✓ No	✓ No
Grounded Segmentation	✓ Human-provided points	✗ No grounding	✓ Text-Grounded

offline human labels to extract precomputed object features, while FTD (Chen et al., 2024) applied prompt-free SAM segmentation and trained a CNN policy on stitched images, limiting flexibility and enforcing a fixed segment count. In contrast, SegDAC computes dynamic object representations online without human labels, grounds EfficientViT-SAM (Zhang et al., 2024) predictions with text inputs, and learns directly from a variable-length sequence of segment embeddings in latent space (table 1).

3 BACKGROUND

Visual reinforcement learning (RL) is commonly formulated as a Partially Observable Markov Decision Process (POMDP) (Littman, 2009), where the agent receives high-dimensional image observations without access to the full environment state. A finite-horizon POMDP is defined by (S, O, A, P, R, γ) , where S is the state space, O the observation space (e.g., RGB images), A the action space, P the unknown transition function, R the reward function, $\gamma \in [0, 1]$ the discount factor, and H the finite horizon of each episode. The objective is to learn a policy $\pi : O \mapsto A$ that maximizes the expected discounted return $\mathbb{E}_\pi \left[\sum_{t=0}^{H-1} \gamma^t r_t \right]$.

We build on the Soft Actor-Critic (SAC) algorithm (Haarnoja et al., 2018; 2019), a widely used actor-critic method for continuous control (Yarats et al., 2020; Laskin et al., 2020; Kostrikov et al., 2021; Hansen & Wang, 2021; Hansen et al., 2021; Bertoin et al., 2023; Yuan et al., 2022; Grooten et al., 2023; Chen et al., 2024; Almuzairee et al., 2024). SAC maximizes both return and policy entropy: the critic minimizes the Bellman residual, while the actor maximizes the critic’s Q-value under the current policy. For the exact mathematical formulation and loss functions, we refer readers to the original SAC papers, since SegDAC uses the vanilla SAC losses during training without modification. Unlike standard visual RL pipelines that stack multiple frames, we extract segment embeddings from a single frame at each time step and process them as a variable-length sequence.

4 METHOD

An overview of SegDAC is shown in Figure 1. Given an RGB image and a set of grounding text inputs, the grounded segmentation module (section 4.1) uses YOLO-World (Cheng et al., 2024) to generate bounding boxes based on the text inputs and EfficientViT-SAM (Zhang et al., 2024) to produce segment masks and patch embeddings. The segment embedding extraction module (section 4.2) extracts features within each mask to form a variable-length sequence of segment embeddings, which is then passed to a transformer-based actor critic (section 4.3) to predict actions/Q-values.

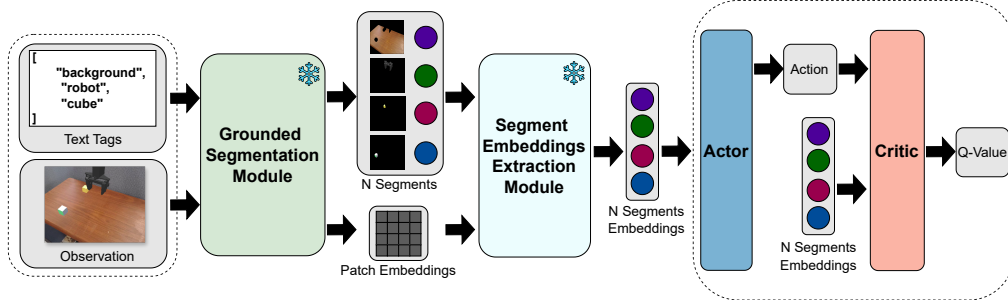


Figure 1: SegDAC overview and components.

Operating directly on segment embeddings enables reasoning over semantically meaningful regions while avoiding pixel-level noise. Further details on the grounded segmentation module and segment embeddings extraction module are provided in the next section. Refer to the appendix for text inputs, definitions, and implementation details.

4.1 GROUNDED SEGMENTATION MODULE

Our grounded segmentation module, shown in Figure 2, is inspired by Grounded SAM (Ren et al., 2024), which combines Grounding DINO (Liu et al., 2024) with SAM (Kirillov et al., 2023) for

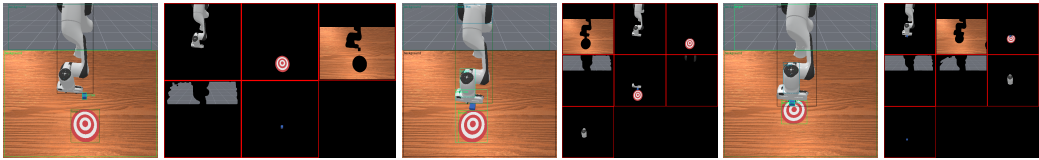


Figure 3: Examples of grounded segments for the PushCube task. Left: image with YOLO-World bounding boxes. Right: segments extracted by EfficientViT-SAM using boxes.

text-guided segmentation. However, we found it too slow for online RL. Instead, we adopt a faster pipeline: YOLO-World (Cheng et al., 2024) generates bounding boxes from an open-vocabulary of simple text inputs and EfficientViT-SAM (Zhang et al., 2024) extracts segments within those boxes. For simplicity, we refer to EfficientViT-SAM as SAM throughout the rest of the paper. A key characteristic of our module is that the number of output segments, N , is variable across different time steps, unlike methods that operate on a fixed number of object representations (Chen et al., 2024; Locatello et al., 2020; Shi et al., 2024; Daniel & Tamar, 2022).

To avoid the inefficiency and randomness of prompt-free segmentation, which relies on dense grids of points and heavy post-processing, we adopt a prompt-based design. YOLO-World, an open-vocabulary detector, predicts K bounding boxes from a list of text tags (e.g., "cube", "apple", "bowl"). The predicted boxes are passed to SAM as prompts, which produces N segments per frame, where N can naturally vary across time. This setup directs SAM toward task-relevant objects and yields more semantically grounded segmentations. The text inputs can be simple object names or small group of words rather than long free-form descriptions, which reduces ambiguity and makes text grounding practical in online RL. They can be defined flexibly: for example, ahead of time per task, shared across tasks, or generated dynamically using external models such as VLMs (Vasu et al., 2025) or image taggers like RAM (Zhang et al., 2023b) and RAM++ (Zhang et al., 2025). For simplicity, we defined task-specific lists in our experiments. These could also be concatenated into a larger list, since YOLO-World is incentivized to output bounding boxes only for objects present in the scene. This means our architecture naturally supports task-agnostic text inputs as well. For efficiency, we reuse the SAM encoder’s patch embeddings, leveraging its pretrained representations (Zhang et al., 2024; Kirillov et al., 2023) and use it to compute segment embeddings in our Segment Embeddings Extraction Module (section 4.2). Both YOLO-World and SAM remain frozen throughout training and inference.

Figures 3 shows examples of the grounded segments extracted for the PushCube-v1 task. While YOLO-World’s predictions are not always perfect, they effectively decompose the scene into bounding boxes based on the text tags. Notably, incorrect label predictions do not affect segmentation quality, as SAM relies only on bounding box coordinates, helping avoid compounding errors.

Motivated by our ablation experiments in Appendix B.1, we also include a generic "background" text tag to encourage detection of additional segments. This helps the agent learn to ignore irrelevant regions and improves generalization compared to using only task-specific tags. The set of text inputs is kept broad and simple, and we did not perform extensive tuning, showing that SegDAC works without careful prompt engineering.

4.2 SEGMENT EMBEDDINGS EXTRACTION MODULE

The segment embedding extraction module takes as input N binary segmentation masks and the patch embeddings from the SAM encoder and outputs N segment embeddings where N varies per frame. This module in Figure 4 has no trainable parameters.

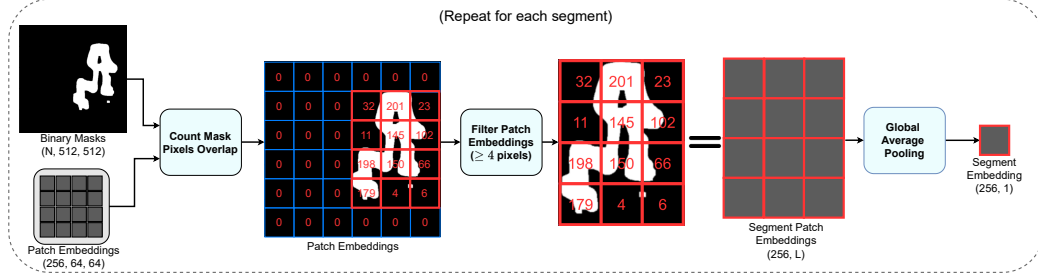


Figure 4: Segment embedding extraction: For each SAM-predicted mask, we select patch embeddings with sufficient overlap (≥ 4 pixels), then apply global average pooling to obtain one embedding per segment.

To compute a segment embedding, we identify the patch embeddings that spatially overlap with the segment’s binary mask. For each patch, we count the number of active (value=1) pixels from the mask within the patch boundary. Patches with fewer than a threshold (e.g.: 4 pixels) are discarded. We then apply global average pooling over the remaining relevant patch embeddings to produce a single embedding vector of dimension S (e.g: $S = 256$). This process is repeated independently for each of the N masks.

An analysis of the segment embedding extraction process including patch overlap heatmap, mask-patch alignment is provided in the appendix (F).

4.3 ACTOR CRITIC NETWORKS

The actor network (Figure 5) maps segment embeddings and proprioceptive inputs to action distribution parameters. It takes a variable set of N segment embeddings of dimension S and proprioceptive inputs of dimension P (we use joint positions for real-world applicability). Both are linearly projected to a shared dimension D , and token type encodings (query, segment, proprioception) are added to help the network distinguish input types.

To encode spatial information, we follow Chen et al. (2025) and compute positional encodings from segment bounding box coordinates via a small learned MLP, which are added to the segment embeddings. The combined segment and proprioceptive tokens form the keys and values for our transformer decoder (Vaswani et al., 2023), while a learned query token serves as the query input.

The decoder uses multi-head cross-attention to contextualize the query, which is then passed through an MLP that outputs a tensor of size $2 \times A$, corresponding to the mean and standard deviation of the action distribution in SAC. The architecture is modular and can be adapted to other algorithms (e.g: TD3) by adjusting the output layer dimension.

The critic network (Figure 5) estimates the Q-value given segment embeddings, proprioceptive information and an action. All of these inputs are each projected to a shared dimension D . Token type encodings are added to all inputs, and segment embeddings receive additional positional encodings via a learned MLP from bounding box coordinates, as in the actor. Segment and proprioception

tokens form the keys (K) and values (V) for the transformer decoder. In contrast to the actor, the action is concatenated with a learned token and passed through an MLP to produce a fused query token. The transformer decoder contextualizes this query, and a final MLP projects the output to a scalar Q-value, compatible with model-free RL algorithms such as SAC, TD3, DQN etc.

5 EXPERIMENTS

We evaluate SegDAC on a new visual generalization benchmark built on ManiSkill3 (Tao et al., 2024), covering 8 manipulation tasks with three difficulty levels (easy, medium, hard) and 12 visual perturbations. This benchmark uses clear criteria rather than random sampling, enabling systematic evaluation. We compare SegDAC with state-of-the-art baselines on sample efficiency and generalization, and further analyze its robustness to segment variability and its segment-level attention patterns. We also provide extensive quantitative and qualitative results, case studies and failure analyses in the appendix (Section A.5), showing how SegDAC performs under strong visual perturbations.

Training and Evaluation Protocol Following prior work in model-free visual RL (Hansen et al., 2021; Almuzairee et al., 2024), all agents were trained for 1M environment steps without perturbations across 8 tasks (Franka Panda arm and Unitree G1 humanoid). Policies were evaluated every 10K steps on unperturbed seeds (10 rollouts, 5 seeds). Hyperparameters were shared across tasks, with only text inputs differing.

Generalization Benchmark To assess visual generalization, we extended ManiSkill3 with 8 tasks, 3 difficulty levels, and up to 12 perturbation types per task. Although DMC-GB (Hansen et al., 2021) has been widely used, Yuan et al. (2023) showed that it does not fully capture the demands of realistic environments. ManiSkill3 offers a stronger basis for robotics simulation, and our benchmark increases the difficulty further by introducing a wide range of visual and semantic perturbations. Each condition was tested with 5 seeds and 50 rollouts, and we report interquartile mean (IQM) returns with 95% confidence intervals following Agarwal et al. (2022). Additional details are provided in the appendix A.

5.1 VISUAL GENERALIZATION BENCHMARK AND RESULTS

Inspired by The Colosseum benchmark (Pumacay et al., 2024), we define the following taxonomy of scene entities:

Manipulation Object (MO): The task-critical object directly grasped or moved by the robot’s end-effector to complete the main objective.

Receiver Object (RO): An essential object not directly manipulated, but necessary for task completion by interacting with the MO.

Primary Interaction Surface (Table): The main horizontal surface that supports or anchors interactions between MOs and ROs.

Background Elements: All other visual components not classified above (e.g., walls, peripheral floor, skybox, distant scenery).

Visual perturbation categories include: (1) camera (pose, field of view), (2) lighting (direction, color), (3) color (MO, RO, table, background) and (4) texture (MO, RO, table, background).

Difficulty levels. Table 2 summarizes the three difficulty levels used in our visual generalization benchmark.

Easy involves minor visual changes that remain close to the default configuration, maintaining high similarity. These serve as smoke tests to verify robustness against small, non-disruptive variations.

Medium introduces substantial visual changes that re-

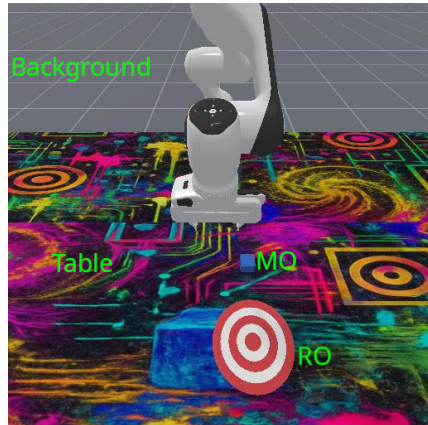


Figure 6: Hard visual perturbation in the PushCube task, with scene entities labeled using our taxonomy.

Table 2: Difficulty levels.

Difficulty	Visual change	Semantic perturbation
Easy	✓ Low	✗ None
Medium	✓ Moderate	✗ None
Hard	✓ High	✓ Present

duce similarity to the default view while remaining task-valid. Perturbations are designed to avoid semantic conflicts between scene entities (for example, avoiding textures or colors that could alter an object’s meaning). These settings are visually distinct yet realistic and solvable.

Hard applies aggressive out-of-distribution perturbations that introduce both visual and semantic challenges. Configurations differ strongly from the default view, with extreme changes in camera angles, lighting, colors, or textures that may confuse perception (for example, a cube textured like the target). They are intentionally difficult and not optimized to facilitate task completion.

For extended details on benchmark definitions as well as quantitative and qualitative results across tasks and perturbations, we refer the reader to Appendix A.

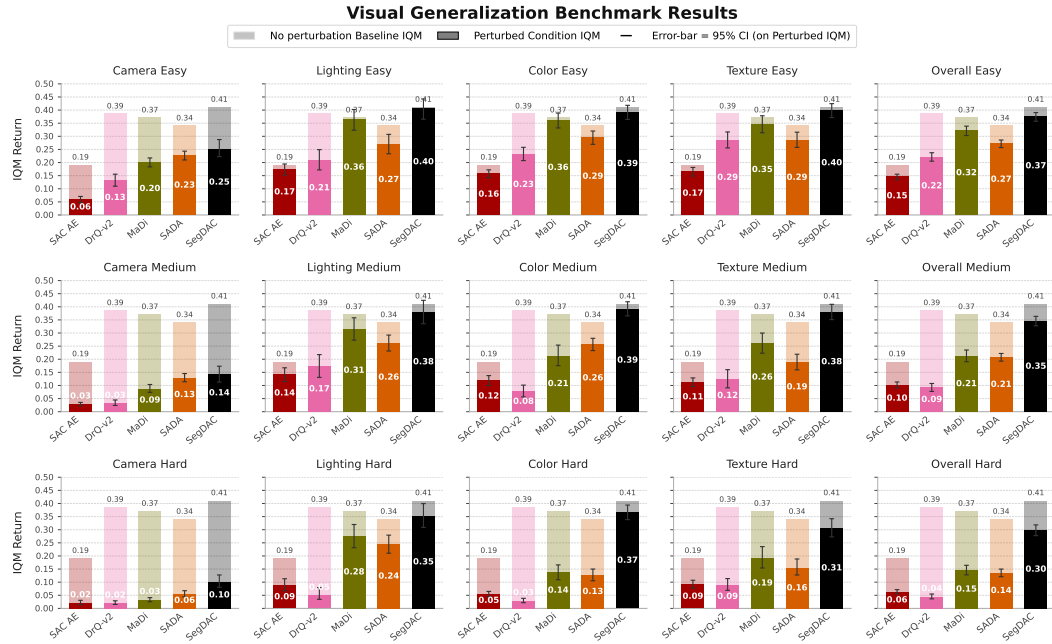


Figure 7: Visual generalization results grouped by categories.

Results: We evaluate four visual RL baselines: SAC-AE (Yarats et al., 2020) as a lower bound, DrQ-v2 (Yarats et al., 2021) as a state-of-the-art in sample efficiency, MaDi (Grooten et al., 2023) and SADA (Almuzairee et al., 2024) as strong methods in visual generalization.

As shown by Figure 7, SegDAC consistently outperforms all baselines across difficulty levels and perturbation categories. While most baselines maintain reasonable performance under easy perturbations, their performance degrades sharply in medium and hard settings. In contrast, SegDAC retains strong performance even under severe distribution shifts. For example, in the hardest setting, MaDi drops from 0.37 to 0.15 IQM (-0.22), while SegDAC only drops from 0.41 to 0.30 (-0.11), achieving approximately twice the performance of both MaDi and SADA. This widening gap highlights the superior robustness of our approach as visual perturbations become more challenging. Although DrQ-v2 remains competitive in terms of sample efficiency (see Figure 11), it shows poor generalization under visual perturbations, with a sharp drop in IQM return even at the easy difficulty level. Notably, all methods struggle in the camera hard setting, suggesting limitations in current single-view architectures. Addressing viewpoint sensitivity through multi-view or viewpoint-invariant approaches is a promising direction for future work.

6 ROBUSTNESS TO IMAGE SEGMENTS VARIABILITY

Figure 8 shows that the number of segments detected by SAM can vary considerably during a rollout. This variability motivates the need for our approach, SegDAC, which can dynamically adjust on the fly to a changing number of segments. **Unlike prior methods, SegDAC is the first model-free online visual RL approach to learn directly from a dynamic sequence of segment embeddings that vary across time, rather than reconstructing images from detected segments or relying**

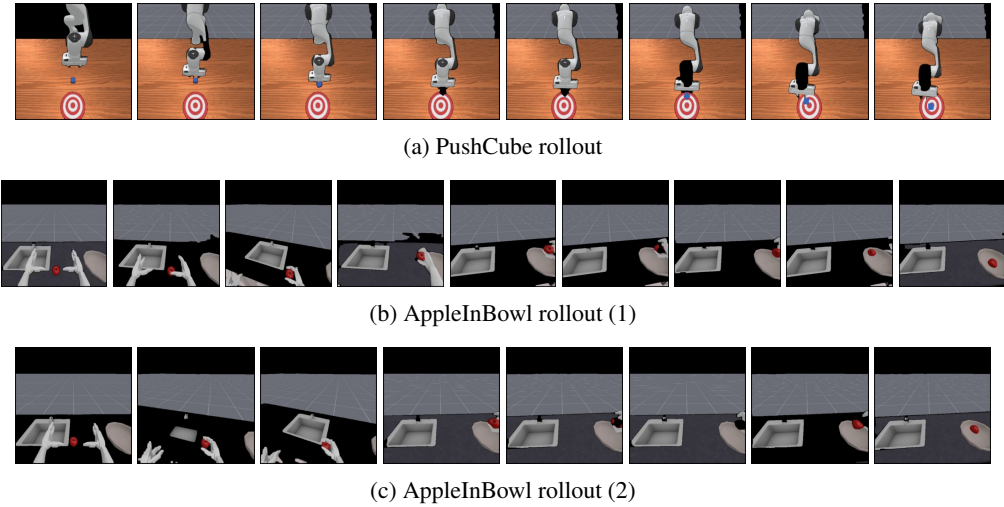


Figure 9: Rollouts showing variability in detected segments. Segments are stitched into one frame at each timestep. Black regions indicate missed detections.

on fixed pre-computed representations. By treating segments as a dynamic sequence instead of fixing their number per task, SegDAC allocates computation adaptively and provides greater representational capacity for complex scenes. In our experiments, we kept the text inputs fixed per task and did not tune SAM parameters or rely on heavy prompt engineering, even though such tuning or using a VLM to generate improved prompts could reduce variability. Nevertheless, a method that is natively robust to dynamic variability is preferred, since the real world is complex and cannot be tuned for in advance, making robustness to variance an important benchmark. Figure 9 presents rollouts where the set of detected segments varies significantly over time, including changes in semantic importance. Note that for visualization, all detected segments are stitched together into a single frame, while SegDAC processes them as a sequence of individual segments. Black regions indicate frames where SAM failed to detect certain objects.

Figure 9 shows that for some rollouts, the background is initially undetected but later appears. The cube, a task-critical object, disappears midway through the trajectory. Part of the robot arm is no longer segmented toward the end. Despite such changes, including the temporary disappearance of task-critical segments like the cube or apple, SegDAC maintains robust behaviour and continues to handle dynamically changing segment inputs effectively.

This robustness is especially important because SegDAC does not rely on temporal smoothing, memory, or frame stacking. In Appendix G, we show additional examples such as temporary occlusions and these are all part of a broader robustness to variability in image segmentation. We hypothesize that this robustness comes from the properties of the segment embeddings combined with training under dynamic object-centric representations. Each embedding is relatively precise, focusing on an object or region, but also enriched with contextual information from the scene through self-attention from SAM’s encoder. Variability in the detected segments and in the number of detected segments forces the policy to learn to use this contextual information. As a result, SegDAC handles inconsistent or incomplete segmentation inputs in a more graceful way.

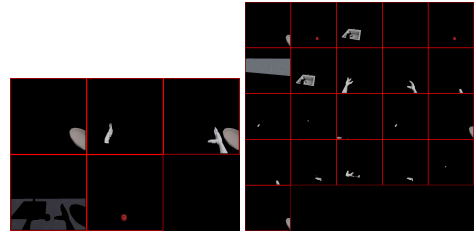


Figure 8: Variability in the number of segments detected by SAM at different time steps in the UnitreeG1PlaceAppleInBowl-v1 task (5 vs 21 segments).

6.1 SEGMENT ATTENTION ANALYSIS

Figure 10, along with extensive qualitative examples in Appendix G, demonstrates that SegDAC selectively attends to task-relevant objects while ignoring irrelevant segments such as the background

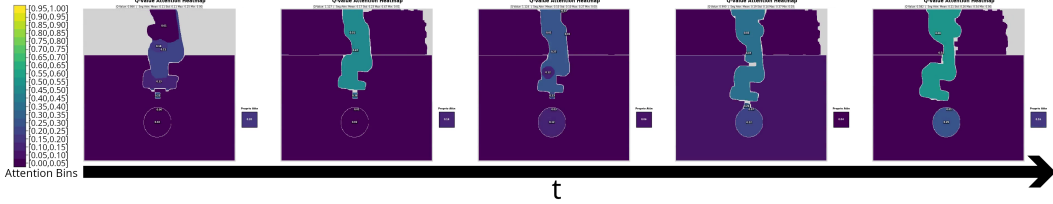


Figure 10: Critic attention on visual segments and proprioception during Q-value prediction.

or the table. Without history or frame stacking, the model adapts its attention over time, it focuses on the robot arm and cube at the start, then shifts toward the target after grasping the cube.

We observe that SegDAC does not maintain uniform attention on the robot throughout the trajectory. In some tasks, the model places more weight on proprioceptive features, while in others it emphasizes the robot arm. The goal is often ignored initially, especially when the first sub-task is to reach or grasp the manipulation object. Once the object is secured and needs to be moved, the model reallocates attention to the goal.

This behavior suggests that allowing the model to learn its own attention distribution leads to more adaptive and flexible decision-making compared to approaches that impose rigid or handcrafted attention patterns.

6.2 SAMPLE EFFICIENCY

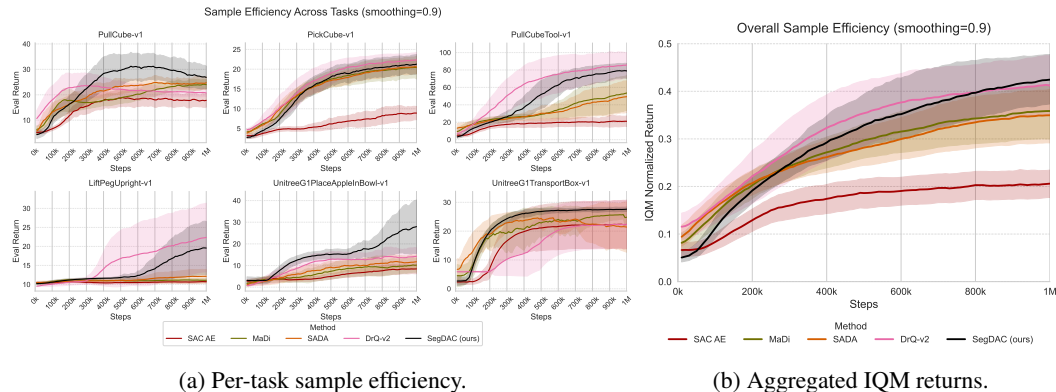


Figure 11: Sample efficiency curves for manipulation tasks and their aggregate. The aggregate shows the IQM normalized return across all 8 tasks and 5 seeds with 95% confidence intervals.

To assess the sample efficiency of SegDAC, we compare it to the same baselines used in the visual generalization benchmark. Figure 11 shows that SegDAC matches the sample efficiency of the previous state-of-the-art DrQ-v2 across all tasks and outperforms it in three out of eight tasks. Moreover, SegDAC consistently achieves higher sample efficiency than the visual generalization baselines (MaDi, SADA) on every task. While methods that excel in sample efficiency often struggle with visual generalization, and methods strong in visual generalization typically sacrifice efficiency, SegDAC challenges this trade-off and demonstrates that it is possible to achieve strong performance in both dimensions. Refer to the appendix (section J) for sample efficiency plots on additional tasks.

7 DISCUSSION

We introduced SegDAC, a novel actor-critic architecture that efficiently integrates pre-trained perception with text-grounded, object-centric segmentation to model relationships among variable image segments. The results are evaluated across multiple manipulation tasks with different robots. SegDAC achieves strong performance without relying on frame stacking, data augmentation, human labels, or auxiliary tasks. While this work focuses on short-horizon online RL, extending SegDAC to longer horizons, alternative learning paradigms and real-world deployment is a promising direction. However, SegDAC improves both visual generalization and sample efficiency and remains robust even when image regions are missing.

REFERENCES

Rishabh Agarwal, Max Schwarzer, Pablo Samuel Castro, Aaron Courville, and Marc G. Bellemare. Deep reinforcement learning at the edge of the statistical precipice, 2022. URL <https://arxiv.org/abs/2108.13264>.

Abdulaziz Almuzairee, Nicklas Hansen, and Henrik I. Christensen. A recipe for unbounded data augmentation in visual reinforcement learning, 2024. URL <https://arxiv.org/abs/2405.17416>.

David Bertoin, Adil Zouitine, Mehdi Zouitine, and Emmanuel Rachelson. Look where you look! saliency-guided q-networks for generalization in visual reinforcement learning, 2023. URL <https://arxiv.org/abs/2209.09203>.

Albert Bou, Matteo Bettini, Sebastian Dittert, Vikash Kumar, Shagun Sodhani, Xiaomeng Yang, Gianni De Fabritiis, and Vincent Moens. Torchrl: A data-driven decision-making library for pytorch, 2023. URL <https://arxiv.org/abs/2306.00577>.

Chao Chen, Jiacheng Xu, Weijian Liao, Hao Ding, Zongzhang Zhang, Yang Yu, and Rui Zhao. Focus-then-decide: Segmentation-assisted reinforcement learning. *Proceedings of the AAAI Conference on Artificial Intelligence*, 38(10):11240–11248, Mar. 2024. doi: 10.1609/aaai.v38i10.29002. URL <https://ojs.aaai.org/index.php/AAAI/article/view/29002>.

Delong Chen, Samuel Cahyawijaya, Jianfeng Liu, Baoyuan Wang, and Pascale Fung. Subobject-level image tokenization, 2025. URL <https://arxiv.org/abs/2402.14327>.

Tianheng Cheng, Lin Song, Yixiao Ge, Wenyu Liu, Xinggang Wang, and Ying Shan. Yolo-world: Real-time open-vocabulary object detection, 2024. URL <https://arxiv.org/abs/2401.17270>.

Tal Daniel and Aviv Tamar. Unsupervised image representation learning with deep latent particles, 2022. URL <https://arxiv.org/abs/2205.15821>.

Alexey Dosovitskiy, Lucas Beyer, Alexander Kolesnikov, Dirk Weissenborn, Xiaohua Zhai, Thomas Unterthiner, Mostafa Dehghani, Matthias Minderer, Georg Heigold, Sylvain Gelly, Jakob Uszkoreit, and Neil Houlsby. An image is worth 16x16 words: Transformers for image recognition at scale, 2021. URL <https://arxiv.org/abs/2010.11929>.

Quentin Garrido, Mahmoud Assran, Nicolas Ballas, Adrien Bardes, Laurent Najman, and Yann LeCun. Learning and leveraging world models in visual representation learning, 2024. URL <https://arxiv.org/abs/2403.00504>.

Bram Grooten, Tristan Tomilin, Gautham Vasan, Matthew E. Taylor, A. Rupam Mahmood, Meng Fang, Mykola Pechenizkiy, and Decebal Constantin Mocanu. Madi: Learning to mask distractions for generalization in visual deep reinforcement learning, 2023. URL <https://arxiv.org/abs/2312.15339>.

Tuomas Haarnoja, Aurick Zhou, Pieter Abbeel, and Sergey Levine. Soft actor-critic: Off-policy maximum entropy deep reinforcement learning with a stochastic actor, 2018. URL <https://arxiv.org/abs/1801.01290>.

Tuomas Haarnoja, Aurick Zhou, Kristian Hartikainen, George Tucker, Sehoon Ha, Jie Tan, Vikash Kumar, Henry Zhu, Abhishek Gupta, Pieter Abbeel, and Sergey Levine. Soft actor-critic algorithms and applications, 2019. URL <https://arxiv.org/abs/1812.05905>.

Nicklas Hansen and Xiaolong Wang. Generalization in reinforcement learning by soft data augmentation, 2021. URL <https://arxiv.org/abs/2011.13389>.

Nicklas Hansen, Hao Su, and Xiaolong Wang. Stabilizing deep q-learning with convnets and vision transformers under data augmentation, 2021. URL <https://arxiv.org/abs/2107.00644>.

Alexander Kirillov, Eric Mintun, Nikhila Ravi, Hanzi Mao, Chloe Rolland, Laura Gustafson, Tete Xiao, Spencer Whitehead, Alexander C. Berg, Wan-Yen Lo, Piotr Dollár, and Ross Girshick. Segment anything, 2023. URL <https://arxiv.org/abs/2304.02643>.

Ilya Kostrikov, Denis Yarats, and Rob Fergus. Image augmentation is all you need: Regularizing deep reinforcement learning from pixels, 2021. URL <https://arxiv.org/abs/2004.13649>.

Mario Michael Krell, Matej Kosec, Sergio P. Perez, and Andrew Fitzgibbon. Efficient sequence packing without cross-contamination: Accelerating large language models without impacting performance, 2022. URL <https://arxiv.org/abs/2107.02027>.

Michael Laskin, Kimin Lee, Adam Stooke, Lerrel Pinto, Pieter Abbeel, and Aravind Srinivas. Reinforcement learning with augmented data, 2020. URL <https://arxiv.org/abs/2004.14990>.

Marion Lepert, Ria Doshi, and Jeannette Bohg. Shadow: Leveraging segmentation masks for zero-shot cross-embodiment policy transfer. In Conference on Robot Learning (CoRL), Munich, Germany, 2024.

Michael L. Littman. A tutorial on partially observable markov decision processes. Journal of Mathematical Psychology, 53(3):119–125, 2009. ISSN 0022-2496. doi: <https://doi.org/10.1016/j.jmp.2009.01.005>. URL <https://www.sciencedirect.com/science/article/pii/S0022249609000042>. Special Issue: Dynamic Decision Making.

Shilong Liu, Zhaoyang Zeng, Tianhe Ren, Feng Li, Hao Zhang, Jie Yang, Qing Jiang, Chunyuan Li, Jianwei Yang, Hang Su, Jun Zhu, and Lei Zhang. Grounding dino: Marrying dino with grounded pre-training for open-set object detection, 2024. URL <https://arxiv.org/abs/2303.05499>.

Francesco Locatello, Dirk Weissenborn, Thomas Unterthiner, Aravindh Mahendran, Georg Heigold, Jakob Uszkoreit, Alexey Dosovitskiy, and Thomas Kipf. Object-centric learning with slot attention, 2020. URL <https://arxiv.org/abs/2006.15055>.

Jiafei Lyu, Le Wan, Xiu Li, and Zongqing Lu. Understanding what affects generalization gap in visual reinforcement learning: Theory and empirical evidence, 2024. URL <https://arxiv.org/abs/2402.02701>.

Andrew Melnik, Augustin Harter, Christian Limberg, Krishan Rana, Niko Suenderhauf, and Helge Ritter. Critic guided segmentation of rewarding objects in first-person views, 2021. URL <https://arxiv.org/abs/2107.09540>.

Volodymyr Mnih, Koray Kavukcuoglu, David Silver, Alex Graves, Ioannis Antonoglou, Daan Wierstra, and Martin Riedmiller. Playing atari with deep reinforcement learning, 2013. URL <https://arxiv.org/abs/1312.5602>.

Adam Paszke, Sam Gross, Francisco Massa, Adam Lerer, James Bradbury, Gregory Chanan, Trevor Killeen, Zeming Lin, Natalia Gimelshein, Luca Antiga, Alban Desmaison, Andreas Köpf, Edward Yang, Zach DeVito, Martin Raison, Alykhan Tejani, Sasank Chilamkurthy, Benoit Steiner, Lu Fang, Junjie Bai, and Soumith Chintala. Pytorch: An imperative style, high-performance deep learning library, 2019. URL <https://arxiv.org/abs/1912.01703>.

Deepak Pathak, Pulkit Agrawal, Alexei A. Efros, and Trevor Darrell. Curiosity-driven exploration by self-supervised prediction, 2017. URL <https://arxiv.org/abs/1705.05363>.

Wilbert Pumacay, Ishika Singh, Jiafei Duan, Ranjay Krishna, Jesse Thomason, and Dieter Fox. The colosseum: A benchmark for evaluating generalization for robotic manipulation, 2024. URL <https://arxiv.org/abs/2402.08191>.

Nikhila Ravi, Valentin Gabeur, Yuan-Ting Hu, Ronghang Hu, Chaitanya Ryali, Tengyu Ma, Haitham Khedr, Roman Rädle, Chloe Rolland, Laura Gustafson, Eric Mintun, Junting Pan, Kalyan Vasudev Alwala, Nicolas Carion, Chao-Yuan Wu, Ross Girshick, Piotr Dollár, and Christoph Feichtenhofer. Sam 2: Segment anything in images and videos, 2024. URL <https://arxiv.org/abs/2408.00714>.

Tianhe Ren, Shilong Liu, Ailing Zeng, Jing Lin, Kunchang Li, He Cao, Jiayu Chen, Xinyu Huang, Yukang Chen, Feng Yan, Zhaoyang Zeng, Hao Zhang, Feng Li, Jie Yang, Hongyang Li, Qing Jiang, and Lei Zhang. Grounded sam: Assembling open-world models for diverse visual tasks, 2024. URL <https://arxiv.org/abs/2401.14159>.

Junyao Shi, Jianing Qian, Yecheng Jason Ma, and Dinesh Jayaraman. Composing pre-trained object-centric representations for robotics from "what" and "where" foundation models, 2024. URL <https://arxiv.org/abs/2404.13474>.

K Sreedhar. Enhancement of images using morphological transformations. *International Journal of Computer Science and Information Technology*, 4(1):33–50, February 2012. ISSN 0975-4660. doi: 10.5121/ijcsit.2012.4103. URL <http://dx.doi.org/10.5121/ijcsit.2012.4103>.

Aravind Srinivas, Michael Laskin, and Pieter Abbeel. Curl: Contrastive unsupervised representations for reinforcement learning, 2020. URL <https://arxiv.org/abs/2004.04136>.

Stone Tao, Fanbo Xiang, Arth Shukla, Yuzhe Qin, Xander Hinrichsen, Xiaodi Yuan, Chen Bao, Xinsong Lin, Yulin Liu, Tse kai Chan, Yuan Gao, Xuanlin Li, Tongzhou Mu, Nan Xiao, Arnav Gurha, Zhiao Huang, Roberto Calandra, Rui Chen, Shan Luo, and Hao Su. Maniskill3: Gpu parallelized robotics simulation and rendering for generalizable embodied ai, 2024. URL <https://arxiv.org/abs/2410.00425>.

Pavan Kumar Anasosalu Vasu, Fartash Faghri, Chun-Liang Li, Cem Koc, Nate True, Albert Antony, Gokul Santhanam, James Gabriel, Peter Grasch, Oncel Tuzel, and Hadi Pouransari. Fastvlm: Efficient vision encoding for vision language models, 2025. URL <https://arxiv.org/abs/2412.13303>.

Ashish Vaswani, Noam Shazeer, Niki Parmar, Jakob Uszkoreit, Llion Jones, Aidan N. Gomez, Łukasz Kaiser, and Illia Polosukhin. Attention is all you need, 2023. URL <https://arxiv.org/abs/1706.03762>.

Xudong Wang, Long Lian, and Stella X. Yu. Unsupervised visual attention and invariance for reinforcement learning, 2021. URL <https://arxiv.org/abs/2104.02921>.

Ziyu Wang, Yanjie Ze, Yifei Sun, Zhecheng Yuan, and Huazhe Xu. Generalizable visual reinforcement learning with segment anything model, 2023. URL <https://arxiv.org/abs/2312.17116>.

Haiping Wu, Khimya Khetarpal, and Doina Precup. Self-supervised attention-aware reinforcement learning. *Proceedings of the AAAI Conference on Artificial Intelligence*, 35(12):10311–10319, May 2021. doi: 10.1609/aaai.v35i12.17235. URL <https://ojs.aaai.org/index.php/AAAI/article/view/17235>.

Denis Yarats, Amy Zhang, Ilya Kostrikov, Brandon Amos, Joelle Pineau, and Rob Fergus. Improving sample efficiency in model-free reinforcement learning from images, 2020. URL <https://arxiv.org/abs/1910.01741>.

Denis Yarats, Rob Fergus, Alessandro Lazaric, and Lerrel Pinto. Mastering visual continuous control: Improved data-augmented reinforcement learning, 2021. URL <https://arxiv.org/abs/2107.09645>.

Zhecheng Yuan, Zhengrong Xue, Bo Yuan, Xueqian Wang, Yi Wu, Yang Gao, and Huazhe Xu. Pre-trained image encoder for generalizable visual reinforcement learning, 2022. URL <https://arxiv.org/abs/2212.08860>.

Zhecheng Yuan, Sizhe Yang, Pu Hua, Can Chang, Kaizhe Hu, and Huazhe Xu. Rl-vigen: A reinforcement learning benchmark for visual generalization, 2023. URL <https://arxiv.org/abs/2307.10224>.

Renrui Zhang, Zhengkai Jiang, Ziyu Guo, Shilin Yan, Junting Pan, Xianzheng Ma, Hao Dong, Peng Gao, and Hongsheng Li. Personalize segment anything model with one shot, 2023a. URL <https://arxiv.org/abs/2305.03048>.

Youcai Zhang, Xinyu Huang, Jinyu Ma, Zhaoyang Li, Zhaochuan Luo, Yanchun Xie, Yuzhuo Qin, Tong Luo, Yaqian Li, Shilong Liu, Yandong Guo, and Lei Zhang. Recognize anything: A strong image tagging model, 2023b. URL <https://arxiv.org/abs/2306.03514>.

Zhuoyang Zhang, Han Cai, and Song Han. Efficientvit-sam: Accelerated segment anything model without accuracy loss, 2024. URL <https://arxiv.org/abs/2402.05008>.

Zilong Zhang, Chujie Qin, Chunle Guo, Yong Zhang, Chao Xue, Ming-Ming Cheng, and Chongyi Li. Ram++: Robust representation learning via adaptive mask for all-in-one image restoration, 2025. URL <https://arxiv.org/abs/2509.12039>.

A VISUAL GENERALIZATION BENCHMARK

A.1 VISUAL PERTURBATION CATEGORIES

Category	Perturbations
Camera	camera pose, camera FOV
Lighting	lighting direction, lighting color
Color	MO color, RO color, table color, ground color
Texture	MO texture, RO texture, table texture, ground texture

Table 3: Perturbation categories and their corresponding visual perturbation tests.

Table 3 lists the visual perturbation categories used in Figure 7.

A.2 MODEL SELECTION

For all methods, we tested the final model (for each seed) after 1 million training steps. Early stopping had no significant effect on results, so using the final checkpoint ensured consistency and simplicity across tests.

A.3 SCORES AGGREGATION

Scores are computed using normalized returns, where each return is divided by the maximum number of steps for the task, yielding values in $[0, 1]$. To compute benchmark returns, we first evaluate baseline performance on the unperturbed tasks by running 50 rollouts per task and per model seed. Each average return (over 50 rollouts) is computed for all $m = 8$ tasks and $n = 5$ seeds, yielding $m \times n = 40$ scores. We then compute the IQM and 95% confidence intervals using stratified bootstrap with 50,000 replications, following Agarwal et al. (2022).

For individual perturbation results (e.g., Table 5), we set $m = 1$ (a single task) and $n = 5$ (seeds), with each score averaged over 50 rollouts. For category-level scores (e.g., Camera Easy, Lighting Easy), m is the total number of perturbation-task combinations in that category. For instance, both the Camera and Lighting categories include two perturbations (Pose/FOV and Direction/Color, respectively) applied to 8 tasks, resulting in $m = 2 \times 8 = 16$.

Some perturbation categories involve a receiving object (RO), such as RO Texture and RO Color in the Texture and Color categories. Tasks that do not include a RO (e.g., LiftPegUpright) cannot be evaluated on these specific perturbations, reducing m by one for those tasks. As a result, the total number of perturbation-task pairs varies across categories depending on RO availability. For both Texture and Color, we obtain $m = 29$ after summing over all tasks while accounting for the presence or absence of ROs. A summary of the number of valid perturbation-task pairs per category, accounting for RO presence, is shown in Table 4.

For the overall scores, we aggregated results across all tasks and all perturbations for each difficulty level, yielding a total of $80 + 80 + 145 + 145 = 450$ test cases per difficulty. We then computed the IQM over these 450 results, providing a robust and reliable evaluation.

Perturbation Category	# Tests ($m \times n$)
Camera	$16 \times 5 = 80$
Lighting	$16 \times 5 = 80$
Color	$29 \times 5 = 145$
Texture	$29 \times 5 = 145$

Table 4: Number of test scores per visual perturbation category.

A.4 DIFFICULTY TEXTURES EXAMPLES

To illustrate the impact of benchmark difficulty on scene appearance, we include Blender renders of selected visual perturbations and full-scene previews for each task. Not all Blender renders are shown, the complete set is available at (anonymized for review). The textures and colors are also task-specific, for example, in the Pick Cube task, the default cube is red and the target is green. Accordingly, the texture perturbations vary in difficulty: the easy texture resembles metallic red (similar to the default), the medium texture is unrelated to either red or green, and the hard texture uses green dots resembling the target to induce confusion.

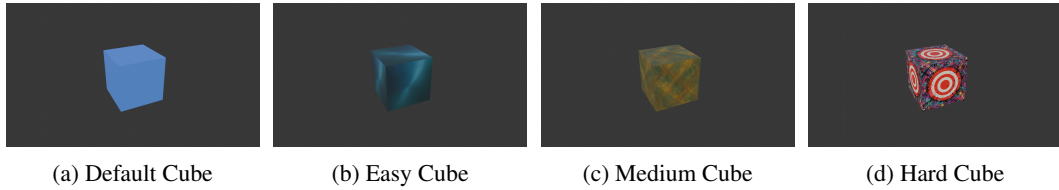


Figure 12: Blender renders for the cube, used in tasks like push/pull/poke cube.

Figure 12 shows how cube appearance changes with perturbation difficulty. The default cube (used when no perturbations are applied) is a solid light blue. The easy texture remains blue with minor variations, such as darker shades and simple patterns, maintaining high visual similarity with the default cube. The medium texture introduces green and yellow-brown tones with slightly more complex patterns, it does not share a lot (if any) visual similarity with the default cube while avoiding conflicts with other scene elements (e.g: robot arm, table, or target). The hard texture is visually and semantically disruptive: it features a chaotic mix of colors and complex patterns, with each cube face displaying a target identical to the task’s actual target. This creates a semantic clash, making it harder for the policy to recognize the cube. These examples demonstrate that our difficulty levels correspond to meaningful and progressively more challenging visual changes.

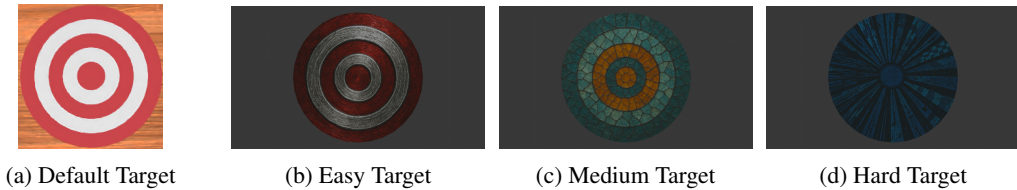
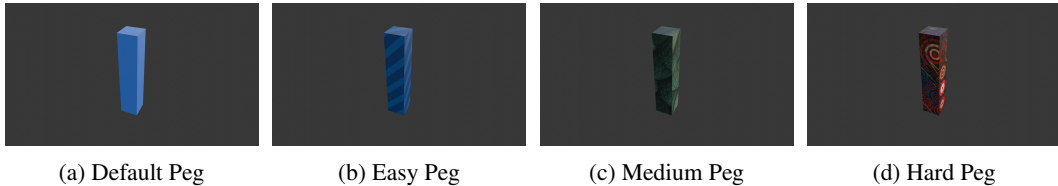


Figure 13: Blender renders for the target.

Figure 13 illustrates the different target textures across difficulty levels. The easy texture closely resembles the default, with red and white nested rings and a slight metallic finish to introduce subtle variation. The medium texture uses entirely different colors and more complex patterns, but retains the same nested ring structure and number of rings. The hard texture is significantly different: it replaces the nested rings with inward-pointing stripes, resembling a dartboard. The color scheme also changes drastically (e.g., blue instead of red), making the target visually and semantically harder to recognize.



(a) Default Peg (b) Easy Peg (c) Medium Peg (d) Hard Peg

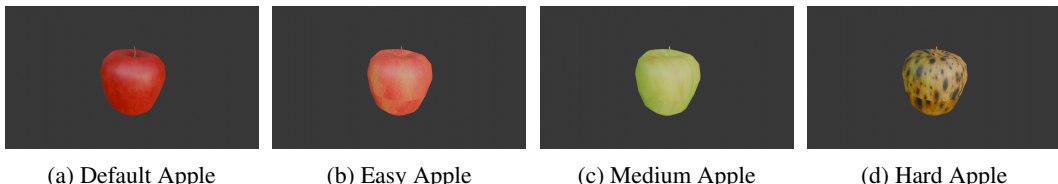
Figure 14: Blender renders for the peg used in the poke cube task.

Figure 14 shows the peg textures across difficulty levels. While multiple tasks include a peg, their textures may differ, the renders shown here are for the poke cube task. The easy texture shares strong visual similarity with the default view, as both are blue. The medium texture uses green, a neutral color that does not resemble any other object in the scene, and features a more complex pattern. The hard texture is visually and semantically distinct, with no similarity to the default. It includes repeated target symbols similar to those used for the task, increasing ambiguity and making the object harder to identify correctly.



(a) Default Tool (b) Easy Tool (c) Medium Tool (d) Hard Tool

Figure 15: Blender renders for the L-shaped tool used in the pull cube tool task.



(a) Default Apple (b) Easy Apple (c) Medium Apple (d) Hard Apple

Figure 16: Blender renders for the apple used in the place apple in the bowl task.

Figure 16 shows the apple textures across difficulty levels. The default apple is a simple red apple. The easy texture is a lighter red with faint orange areas, maintaining strong visual similarity. The medium texture is green, representing a common apple variety, but differing in color. The hard texture shows a brownish, rotten apple that is both visually distinct and semantically less typical, representing a rare case that may be underrepresented in real-world data or training distributions.



(a) Default Box (b) Easy Box (c) Medium Box (d) Hard Box

Figure 17: Blender renders for the box used in the transport box task.

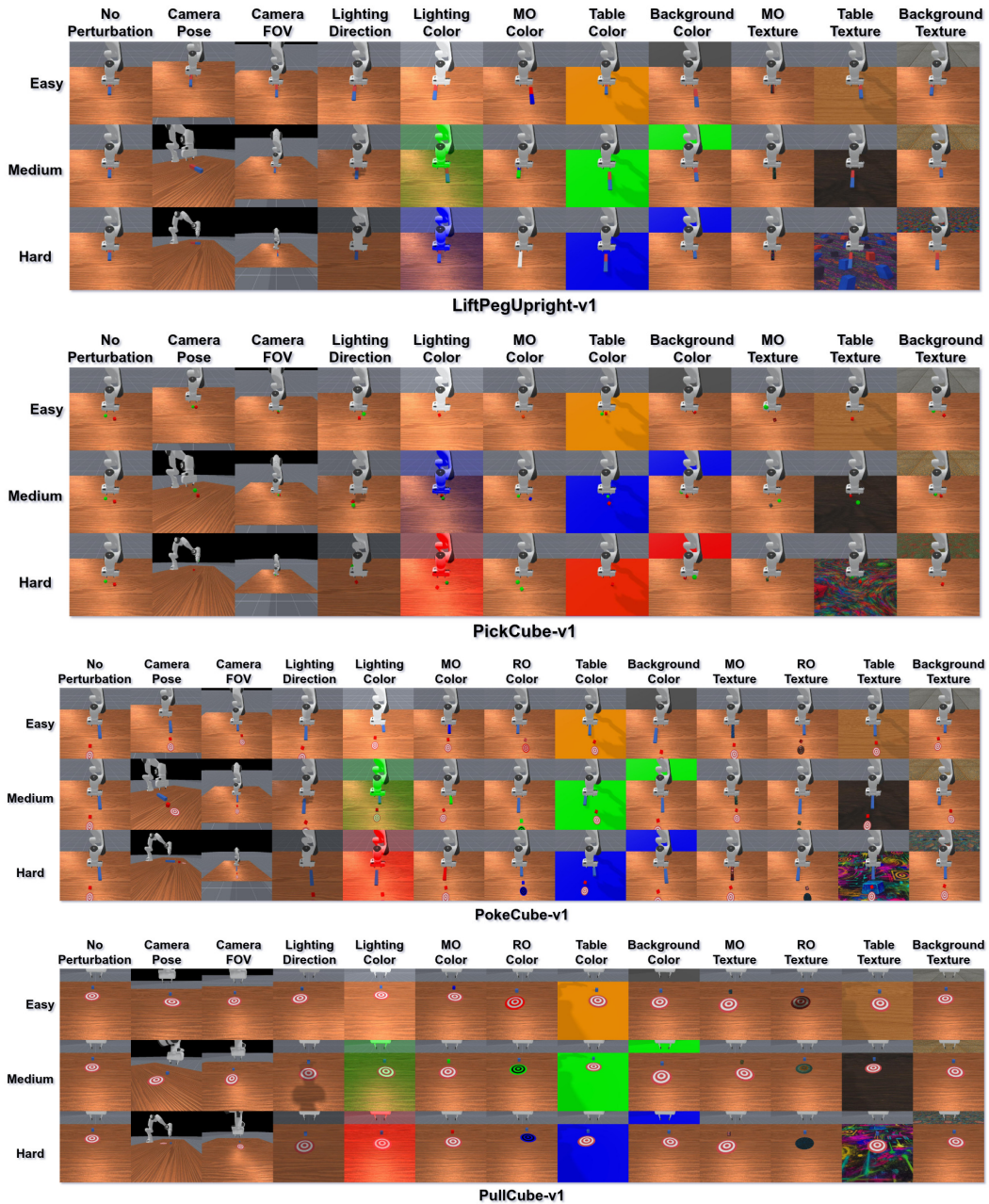


Figure 18: (Part 1) Visual perturbations for all tasks and difficulties.

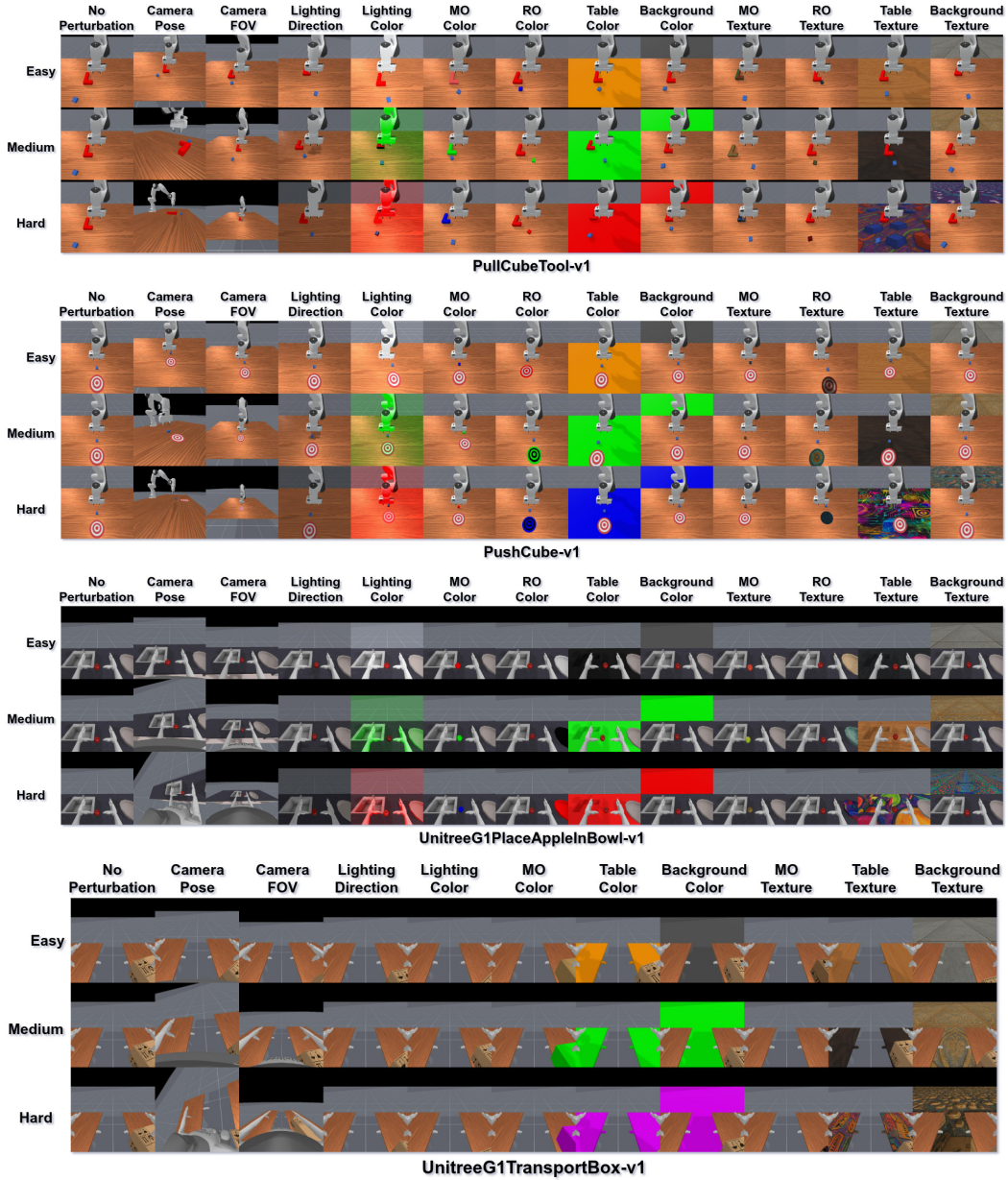


Figure 19: (Part 2) Visual perturbations for all tasks and difficulties.

Figures 18 and 19 show all visual perturbations for each task alongside their default (unperturbed) views. As difficulty increases, observations become more out-of-distribution and challenging. Notably, our camera pose perturbations are more aggressive than those typically used in other benchmarks, making them especially difficult for policies to handle. While no benchmark is perfect, we believe that exposing policies to strong perturbations provides a clearer understanding of their true robustness and generalization capabilities.

A.5 CASE STUDY & FAILURE CASES

Below are qualitative rollout examples comparing SegDAC to MaDi across various tasks and perturbations. We also include cases with camera pose perturbations, as they were the most challenging for all methods.

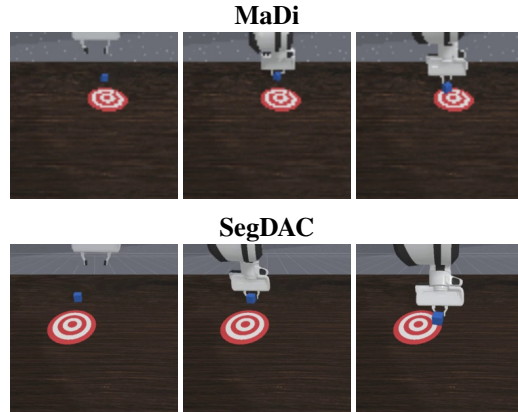


Figure 20: Rollout for *PullCube* - Medium Table Texture (top: MaDi, bottom: SegDAC).

Figure 20 shows that both MaDi and SegDAC are able to successfully complete the Pull Cube task under the medium table texture perturbation (success is reaching the first white ring), regardless of the target’s initial position. This highlights that, in some cases, policies can still succeed under medium-level perturbations and do not always collapse when faced with moderate visual changes.

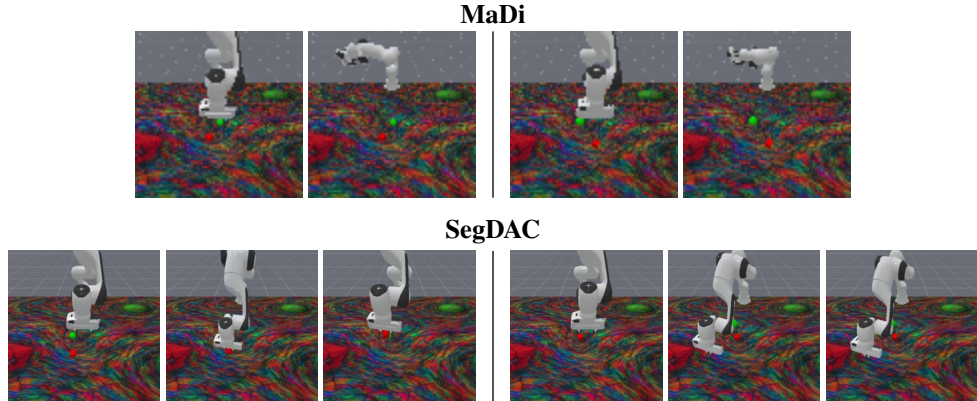


Figure 21: 2 Rollouts for *PickCube* - Hard Table Texture (top: MaDi, bottom: SegDAC).

Figure 21 shows the Pick Cube task under the challenging hard table texture, which includes complex patterns along with a red cube and green target embedded in the texture. This creates significant ambiguity, as the policy may confuse the textured cube with the actual object. MaDi consistently fails, often producing extreme and unstable actions. In contrast, SegDAC succeeds in some rollouts and fails in others. Its failures are more controlled, typically resulting from missed grasp attempts rather than erratic behavior.

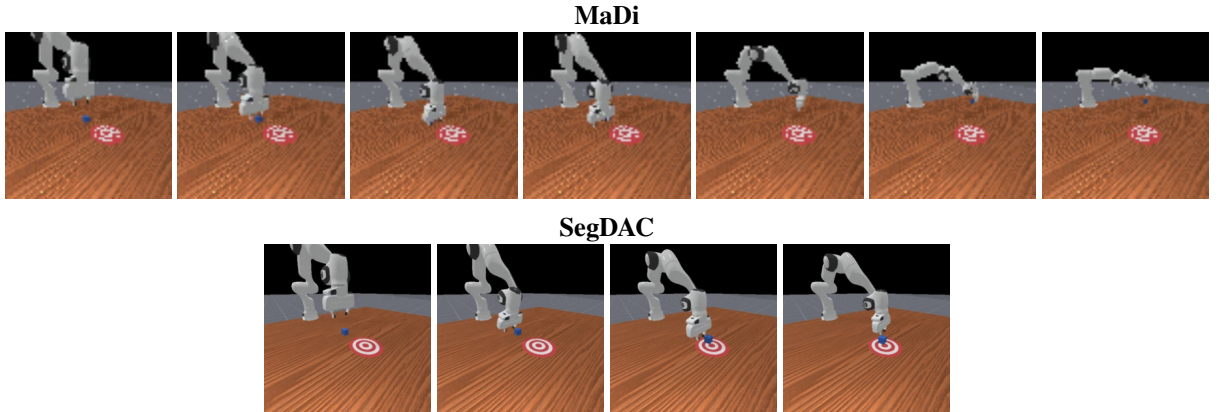


Figure 22: Rollout for *PushCube* - Medium Camera Pose (top: MaDi, bottom: SegDAC).

Figure 22 shows a rollout of the Push Cube task under the medium camera pose perturbation for both MaDi and SegDAC. MaDi initially behaves reasonably by reaching toward the cube, but fails to position the arm correctly. This leads to accumulating errors and eventually to unstable actions that push the cube away from the target. In contrast, SegDAC handles the perturbation more effectively and often succeeds, showing more stable and goal-directed behavior.

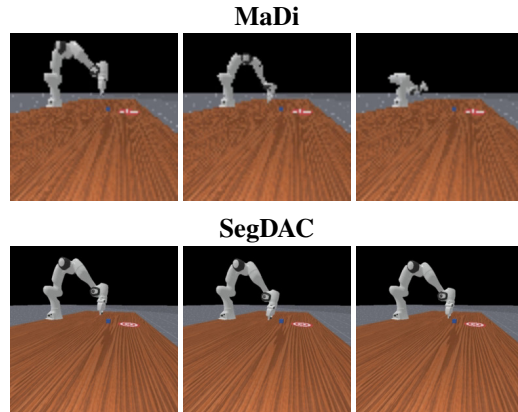


Figure 23: Rollout for *PushCube* - Hard Camera Pose (top: MaDi, bottom: SegDAC).

Figure 23 illustrates the difficulty of the hard camera pose perturbation for both policies. MaDi consistently collapses and produces erratic, non-sensical actions. While SegDAC does not succeed either, it shows more structured behavior, making small back-and-forth motions in an attempt to push the cube. However, it lacks the precision needed and repeatedly misses the cube by a small margin.

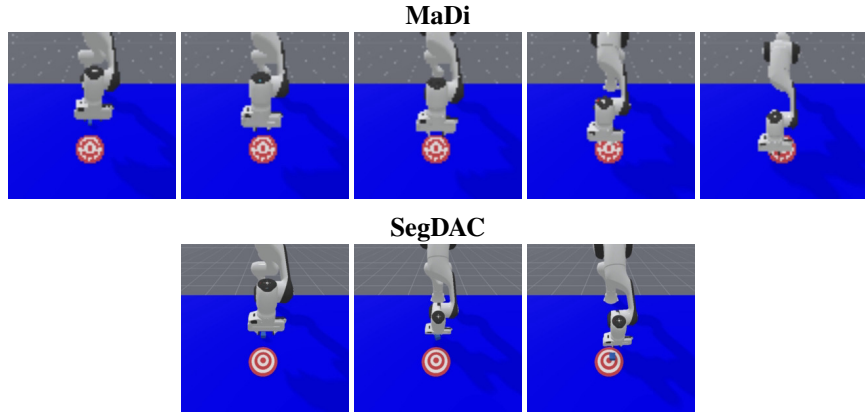


Figure 24: Rollout for *PushCube* - Hard Table Color (top: MaDi, bottom: SegDAC).

Figure 24 shows a rollout of the Push Cube task under the hard table color perturbation. In this case, the table is blue, the same color as the cube, which appears to confuse MaDi. The policy behaves as if the cube is already between the gripper and moves toward the target, while the actual cube remains at its initial position. This issue does not occur with SegDAC, which accurately identifies the cube and pushes it to the center of the target. This highlights the strength of object-centric approaches. While MaDi reasons at the pixel level, SegDAC decomposes the scene into segments and leverages bounding box coordinates of the cube segment to guide the policy more effectively.

A.6 EXHAUSTIVE RESULTS

Table 5 and the subsequent tables report IQM returns and 95% confidence intervals for each visual perturbation, across all tasks, methods, and difficulty levels. The method with the highest absolute IQM return is shown in **bold**, while the method with the best relative improvement over its no-perturbation baseline is underlined. We also include the relative delta between the baseline (no perturbation) IQM return and the return under the perturbed setting. For example, a value of (-2.5%) indicates a 2.5% performance drop compared to the no perturbation case.

Table 5: Easy Camera Fov Test

Task	SAC AE	DrQ-v2	MaDi	SADA	SegDAC
LiftPegUpright	0.20±0.00 (-7.8%)	0.23±0.09 (-50.3%)	0.22±0.01 (-0.3%)	0.22±0.01 (-1.1%)	0.27±0.08 (-34.4%)
PickCube	0.07±0.01 (-60.1%)	0.12±0.04 (-74.0%)	0.14±0.04 (-68.9%)	0.26±0.08 (-32.0%)	0.21±0.02 (-36.5%)
PokeCube	0.06±0.02 (-60.8%)	0.15±0.03 (-66.2%)	0.11±0.01 (-72.9%)	0.14±0.01 (-63.4%)	0.18±0.01 (-55.0%)
PullCube	0.09±0.03 (-76.5%)	0.09±0.06 (-76.0%)	0.42±0.17 (-15.6%)	0.42±0.14 (-13.6%)	0.32±0.12 (-35.7%)
PullCubeTool	0.05±0.03 (-76.8%)	0.12±0.20 (-80.6%)	0.21±0.03 (-65.9%)	0.26±0.10 (-28.3%)	0.63±0.13 (-14.2%)
PushCube	0.12±0.03 (-59.0%)	0.17±0.04 (-62.6%)	0.16±0.02 (-65.3%)	0.24±0.04 (-47.5%)	0.59±0.10 (+30.3%)
PlaceAppleInBowl	0.04±0.01 (-52.5%)	0.11±0.05 (-32.6%)	0.09±0.04 (-29.3%)	0.10±0.04 (-14.2%)	0.21±0.11 (-32.8%)
TransportBox	0.03±0.02 (-31.8%)	0.26±0.07 (-0.7%)	0.26±0.01 (-0.3%)	0.22±0.10 (-9.7%)	0.27±0.01 (-2.5%)

Table 6: Easy Camera Pose Test

Task	SAC AE	DrQ-v2	MaDi	SADA	SegDAC
LiftPegUpright	0.19±0.00 (-11.9%)	0.23±0.09 (-50.5%)	0.20±0.02 (-9.1%)	0.22±0.04 (-1.9%)	0.19±0.00 (-54.0%)
PickCube	0.05±0.02 (-74.9%)	0.07±0.10 (-85.2%)	0.27±0.09 (-39.5%)	0.25±0.06 (-34.5%)	0.12±0.05 (-65.5%)
PokeCube	0.03±0.01 (-83.8%)	0.02±0.01 (-94.6%)	0.16±0.01 (-60.2%)	0.22±0.04 (-42.1%)	0.13±0.02 (-66.7%)
PullCube	0.05±0.03 (-86.1%)	0.02±0.02 (-94.2%)	0.24±0.02 (-51.2%)	0.24±0.05 (-50.1%)	0.35±0.13 (-30.4%)
PullCubeTool	0.02±0.02 (-88.7%)	0.15±0.07 (-76.4%)	0.20±0.05 (-67.6%)	0.22±0.04 (-39.5%)	0.59±0.18 (-20.7%)
PushCube	0.06±0.05 (-80.1%)	0.08±0.06 (-81.4%)	0.30±0.09 (-36.0%)	0.36±0.04 (-21.5%)	0.10±0.11 (-77.3%)
PlaceAppleInBowl	0.03±0.02 (-59.1%)	0.15±0.02 (-11.3%)	0.12±0.06 (-3.5%)	0.12±0.04 (-2.4%)	0.22±0.08 (-29.7%)
TransportBox	0.04±0.04 (-12.6%)	0.26±0.07 (-1.2%)	0.26±0.02 (-0.5%)	0.22±0.10 (-10.5%)	0.28±0.01 (-1.3%)

Table 7: Easy Ground Color Test

Task	SAC AE	DrQ-v2	MaDi	SADA	SegDAC
LiftPegUpright	0.21±0.00 (-0.7%)	0.36±0.12 (-23.0%)	0.23±0.01 (+2.5%)	0.22±0.03 (+0.4%)	0.39±0.15 (-5.5%)
PickCube	0.12±0.01 (-33.7%)	0.13±0.09 (-72.5%)	0.43±0.06 (-2.4%)	0.41±0.03 (+4.7%)	0.35±0.04 (+3.1%)
PokeCube	0.16±0.02 (-0.5%)	0.20±0.12 (-53.3%)	0.41±0.01 (-0.1%)	0.37±0.07 (-3.8%)	0.34±0.06 (-12.1%)
PullCube	0.23±0.04 (-38.7%)	0.13±0.10 (-63.6%)	0.46±0.06 (-6.8%)	0.45±0.18 (-8.5%)	0.51±0.06 (+1.4%)
PullCubeTool	0.19±0.05 (-12.2%)	0.36±0.35 (-42.6%)	0.61±0.20 (-1.4%)	0.36±0.14 (-1.8%)	0.69±0.14 (-7.3%)
PushCube	0.21±0.03 (-29.2%)	0.32±0.16 (-28.9%)	0.44±0.09 (-4.1%)	0.46±0.02 (-0.1%)	0.44±0.04 (-1.8%)
PlaceAppleInBowl	0.08±0.02 (+7.0%)	0.15±0.02 (-8.5%)	0.12±0.05 (+1.0%)	0.11±0.04 (-3.9%)	0.29±0.15 (-9.7%)
TransportBox	<u>0.05±0.04 (+9.2%)</u>	0.24±0.08 (-5.7%)	0.26±0.00 (+0.1%)	0.22±0.10 (-11.9%)	0.28±0.01 (-0.1%)

Table 8: Easy Ground Texture Test

Task	SAC AE	DrQ-v2	MaDi	SADA	SegDAC
LiftPegUpright	0.21±0.01 (-1.3%)	0.46±0.18 (-2.8%)	0.22±0.01 (+1.6%)	0.23±0.03 (+1.6%)	0.42±0.15 (+1.9%)
PickCube	0.10±0.04 (-45.5%)	0.44±0.03 (-4.8%)	0.43±0.06 (-1.9%)	0.40±0.03 (+3.8%)	0.35±0.05 (+5.2%)
PokeCube	0.15±0.02 (-10.8%)	0.43±0.06 (-0.4%)	0.41±0.01 (-1.1%)	0.37±0.07 (-3.9%)	0.40±0.05 (+0.8%)
PullCube	0.25±0.03 (-32.4%)	0.37±0.05 (-0.1%)	0.48±0.03 (-2.5%)	0.42±0.15 (-13.2%)	0.53±0.06 (+4.9%)
PullCubeTool	0.19±0.06 (-15.4%)	0.62±0.17 (-0.6%)	0.61±0.21 (-1.9%)	0.34±0.17 (-8.3%)	0.74±0.16 (-0.6%)
PushCube	0.21±0.03 (-30.1%)	0.34±0.22 (-24.6%)	0.46±0.07 (+0.2%)	0.45±0.01 (-1.8%)	0.46±0.04 (+2.9%)
PlaceAppleInBowl	0.07±0.02 (-3.9%)	0.05±0.04 (-66.8%)	0.12±0.04 (+0.2%)	0.12±0.05 (-2.7%)	0.30±0.17 (-4.7%)
TransportBox	0.03±0.04 (-41.3%)	0.26±0.07 (+1.1%)	0.26±0.00 (-0.0%)	0.21±0.10 (-13.1%)	0.28±0.01 (-0.4%)

Table 9: Easy Lighting Color Test

Task	SAC AE	DrQ-v2	MaDi	SADA	SegDAC
LiftPegUpright	0.21±0.01 (-0.6%)	0.21±0.02 (-54.6%)	0.22±0.02 (+2.3%)	0.21±0.01 (-4.2%)	0.41±0.15 (+0.2%)
PickCube	0.16±0.04 (-13.6%)	0.07±0.04 (-84.8%)	0.43±0.06 (-3.0%)	0.21±0.07 (-46.4%)	0.24±0.05 (-28.9%)
PokeCube	0.16±0.02 (-5.7%)	0.10±0.05 (-76.9%)	0.41±0.01 (-0.8%)	0.17±0.04 (-55.1%)	0.36±0.03 (-7.8%)
PullCube	0.30±0.04 (-19.7%)	0.09±0.05 (-76.1%)	0.49±0.05 (-1.0%)	0.44±0.14 (-9.0%)	0.51±0.05 (+0.8%)
PullCubeTool	<u>0.24±0.07 (+8.2%)</u>	0.09±0.07 (-85.9%)	0.61±0.19 (-2.2%)	0.19±0.10 (-47.4%)	<u>0.72±0.12 (-2.9%)</u>
PushCube	0.26±0.02 (-12.8%)	0.16±0.06 (-64.5%)	0.44±0.07 (-4.7%)	0.37±0.11 (-18.8%)	0.48±0.02 (+5.8%)
PlaceAppleInBowl	0.08±0.03 (+12.3%)	0.04±0.06 (-75.6%)	0.12±0.04 (-6.0%)	0.11±0.06 (-9.9%)	0.32±0.17 (+0.0%)
TransportBox	<u>0.05±0.03 (+3.3%)</u>	0.26±0.07 (-0.6%)	0.26±0.01 (+0.1%)	0.24±0.09 (-0.7%)	0.28±0.01 (+0.0%)

Table 10: Easy Lighting Direction Test

Task	SAC AE	DrQ-v2	MaDi	SADA	SegDAC
LiftPegUpright	0.21±0.01 (-0.2%)	0.46±0.18 (-1.7%)	0.23±0.02 (+2.5%)	0.22±0.03 (+0.9%)	0.40±0.15 (-2.6%)
PickCube	0.17±0.03 (-8.8%)	0.42±0.04 (-8.4%)	0.41±0.05 (-6.0%)	0.38±0.04 (-1.0%)	0.33±0.04 (-2.9%)
PokeCube	0.16±0.03 (-1.8%)	0.39±0.04 (-10.5%)	0.41±0.02 (+0.8%)	0.38±0.08 (-1.9%)	0.40±0.03 (+2.9%)
PullCube	0.17±0.01 (-54.7%)	0.26±0.05 (-30.3%)	0.54±0.07 (+9.6%)	0.55±0.24 (+12.0%)	0.52±0.09 (+4.0%)
PullCubeTool	0.19±0.06 (-11.0%)	0.37±0.22 (-40.4%)	<u>0.62±0.21 (-1.2%)</u>	0.33±0.14 (-9.4%)	0.71±0.12 (-4.6%)
PushCube	0.27±0.03 (-7.7%)	0.46±0.22 (-0.1%)	<u>0.43±0.07 (-6.9%)</u>	0.48±0.02 (+4.7%)	0.45±0.04 (+0.0%)
PlaceAppleInBowl	<u>0.08±0.02 (+4.2%)</u>	0.14±0.03 (-12.0%)	0.11±0.05 (-8.2%)	0.12±0.04 (+0.2%)	0.32±0.17 (+1.7%)
TransportBox	<u>0.05±0.03 (+0.8%)</u>	0.26±0.07 (-0.5%)	0.26±0.01 (+0.1%)	0.24±0.09 (-0.3%)	0.28±0.01 (-0.1%)

Table 11: Easy Mo Color Test

Task	SAC AE	DrQ-v2	MaDi	SADA	SegDAC
LiftPegUpright	0.21±0.01 (-1.3%)	0.27±0.09 (-42.1%)	0.22±0.01 (-0.1%)	0.22±0.02 (-0.8%)	0.40±0.15 (-2.5%)
PickCube	0.14±0.03 (-22.0%)	0.25±0.06 (-45.0%)	0.43±0.06 (-2.9%)	0.31±0.06 (-20.1%)	0.28±0.06 (-17.4%)
PokeCube	0.13±0.02 (-24.1%)	0.17±0.01 (-60.0%)	0.39±0.01 (-4.4%)	0.30±0.05 (-22.1%)	0.40±0.03 (+2.2%)
PullCube	0.24±0.04 (-34.2%)	0.22±0.02 (-39.7%)	0.45±0.02 (-7.6%)	0.34±0.12 (-31.3%)	<u>0.48±0.08 (-3.7%)</u>
PullCubeTool	0.14±0.02 (-38.2%)	0.26±0.16 (-58.9%)	<u>0.50±0.15 (-19.1%)</u>	0.31±0.13 (-14.2%)	0.81±0.17 (+9.8%)
PushCube	0.20±0.03 (-32.0%)	0.23±0.16 (-48.7%)	0.43±0.07 (-6.4%)	0.33±0.13 (-29.1%)	<u>0.45±0.05 (-0.2%)</u>
PlaceAppleInBowl	0.07±0.01 (-7.7%)	0.08±0.04 (-53.4%)	<u>0.13±0.04 (+4.5%)</u>	0.09±0.04 (-21.7%)	0.32±0.17 (+1.0%)
TransportBox	0.05±0.03 (-1.0%)	0.26±0.07 (-0.6%)	<u>0.26±0.01 (-0.0%)</u>	0.24±0.09 (-2.2%)	0.28±0.01 (-0.4%)

Table 12: Easy Mo Texture Test

Task	SAC AE	DrQ-v2	MaDi	SADA	SegDAC
LiftPegUpright	0.20±0.01 (-5.7%)	0.22±0.02 (-52.8%)	0.20±0.01 (-6.8%)	0.22±0.02 (-2.6%)	0.31±0.09 (-23.8%)
PickCube	<u>0.14±0.01 (-22.9%)</u>	0.24±0.05 (-48.0%)	0.23±0.08 (-46.6%)	<u>0.17±0.05 (-57.3%)</u>	0.16±0.02 (-50.9%)
PokeCube	0.12±0.01 (-25.2%)	0.17±0.04 (-61.8%)	0.38±0.03 (-8.1%)	0.22±0.03 (-42.3%)	0.36±0.03 (-8.2%)
PullCube	0.25±0.03 (-32.6%)	0.27±0.05 (-27.1%)	0.47±0.05 (-5.1%)	0.37±0.02 (-24.3%)	0.46±0.10 (-8.5%)
PullCubeTool	0.13±0.05 (-42.0%)	0.12±0.07 (-80.5%)	0.23±0.08 (-63.7%)	0.11±0.14 (-68.9%)	0.35±0.08 (-53.1%)
PushCube	0.18±0.02 (-38.9%)	0.18±0.10 (-59.5%)	0.22±0.16 (-51.9%)	0.19±0.04 (-57.9%)	0.48±0.08 (+7.3%)
PlaceAppleInBowl	0.08±0.02 (+8.5%)	0.15±0.02 (-7.6%)	0.12±0.05 (-5.3%)	0.12±0.04 (-1.2%)	0.29±0.17 (-8.2%)
TransportBox	<u>0.05±0.03 (+4.5%)</u>	0.26±0.07 (-1.1%)	0.26±0.01 (+0.1%)	0.24±0.09 (-3.5%)	0.28±0.01 (+0.0%)

Table 13: Easy Ro Color Test

Task	SAC AE	DrQ-v2	MaDi	SADA	SegDAC
LiftPegUpright	N/A	N/A	N/A	N/A	N/A
PickCube	N/A	N/A	N/A	N/A	N/A
PokeCube	0.17 \pm 0.03 (+0.8%)	0.42\pm0.05 (-3.7%)	0.40 \pm 0.01 (-2.3%)	0.38 \pm 0.08 (-1.2%)	0.40 \pm 0.02 (+1.8%)
PullCube	0.34 \pm 0.06 (-8.7%)	0.29 \pm 0.08 (-20.3%)	0.50\pm0.05 (+1.1%)	0.41 \pm 0.11 (-16.6%)	0.51\pm0.09 (+1.0%)
PullCubeTool	0.18 \pm 0.06 (-15.4%)	0.48 \pm 0.21 (-22.4%)	0.60\pm0.18 (-3.5%)	0.30 \pm 0.16 (-18.6%)	0.70\pm0.14 (-5.9%)
PushCube	0.26 \pm 0.03 (-13.1%)	0.23 \pm 0.22 (-48.8%)	0.43 \pm 0.07 (-6.3%)	0.43 \pm 0.04 (-6.8%)	0.44\pm0.04 (-2.9%)
PlaceAppleInBowl	0.08\pm0.03 (+6.9%)	0.11 \pm 0.02 (-32.4%)	0.12 \pm 0.05 (-0.7%)	0.12 \pm 0.04 (+0.2%)	0.29\pm0.14 (-7.0%)
TransportBox	N/A	N/A	N/A	N/A	N/A

Table 14: Easy Ro Texture Test

Task	SAC AE	DrQ-v2	MaDi	SADA	SegDAC
LiftPegUpright	N/A	N/A	N/A	N/A	N/A
PickCube	N/A	N/A	N/A	N/A	N/A
PokeCube	0.17 \pm 0.04 (+0.9%)	0.35 \pm 0.04 (-19.5%)	0.41\pm0.01 (-0.0%)	0.38 \pm 0.07 (-2.1%)	0.40 \pm 0.04 (+2.0%)
PullCube	0.35 \pm 0.03 (-6.0%)	0.14 \pm 0.12 (-63.0%)	0.58 \pm 0.07 (+17.4%)	0.70\pm0.05 (+43.4%)	0.55 \pm 0.07 (+9.1%)
PullCubeTool	0.20 \pm 0.07 (-6.8%)	0.57 \pm 0.26 (-8.2%)	0.63 \pm 0.20 (+1.2%)	0.35 \pm 0.13 (-3.6%)	0.72\pm0.12 (-2.3%)
PushCube	0.24 \pm 0.03 (-19.4%)	0.33 \pm 0.23 (-28.4%)	0.56 \pm 0.13 (+19.8%)	0.57\pm0.07 (+22.9%)	0.49 \pm 0.05 (+10.0%)
PlaceAppleInBowl	0.06 \pm 0.02 (-20.5%)	0.06 \pm 0.04 (-63.9%)	0.12\pm0.05 (-3.2%)	0.11\pm0.04 (-3.2%)	0.23\pm0.12 (-25.7%)
TransportBox	N/A	N/A	N/A	N/A	N/A

Table 15: Easy Table Color Test

Task	SAC AE	DrQ-v2	MaDi	SADA	SegDAC
LiftPegUpright	0.21 \pm 0.00 (-2.3%)	0.21 \pm 0.02 (-55.3%)	0.21 \pm 0.01 (-6.2%)	0.22 \pm 0.03 (-1.3%)	0.28\pm0.08 (-32.2%)
PickCube	0.06 \pm 0.05 (-68.1%)	0.05 \pm 0.11 (-88.7%)	0.43\pm0.06 (-2.1%)	0.26 \pm 0.07 (-32.7%)	0.19 \pm 0.04 (-43.0%)
PokeCube	0.14 \pm 0.02 (-16.5%)	0.30 \pm 0.14 (-32.1%)	0.40\pm0.01 (-3.5%)	0.28 \pm 0.07 (-28.4%)	0.24 \pm 0.02 (-38.6%)
PullCube	0.14 \pm 0.07 (-63.2%)	0.30 \pm 0.22 (-18.0%)	0.39 \pm 0.14 (-21.6%)	0.42\pm0.03 (-13.3%)	0.42\pm0.05 (-15.7%)
PullCubeTool	0.19 \pm 0.06 (-14.6%)	0.61\pm0.17 (-1.4%)	0.43 \pm 0.28 (-31.6%)	0.35 \pm 0.18 (-5.1%)	0.48 \pm 0.12 (-35.4%)
PushCube	0.24 \pm 0.06 (-19.2%)	0.39 \pm 0.25 (-14.8%)	0.45 \pm 0.08 (-2.2%)	0.45 \pm 0.05 (-3.4%)	0.66\pm0.08 (+46.3%)
PlaceAppleInBowl	0.06 \pm 0.04 (-13.1%)	0.09 \pm 0.04 (-44.1%)	0.12 \pm 0.06 (-6.3%)	0.10 \pm 0.05 (-15.9%)	0.30\pm0.16 (-5.0%)
TransportBox	0.06 \pm 0.03 (+17.4%)	0.19 \pm 0.11 (-25.8%)	0.26 \pm 0.00 (-0.2%)	0.24 \pm 0.09 (-3.7%)	0.28\pm0.01 (-0.5%)

Table 16: Easy Table Texture Test

Task	SAC AE	DrQ-v2	MaDi	SADA	SegDAC
LiftPegUpright	0.21 \pm 0.00 (+0.2%)	0.40\pm0.19 (-15.7%)	0.23\pm0.01 (+2.5%)	0.22 \pm 0.05 (+0.6%)	0.39 \pm 0.13 (-5.4%)
PickCube	0.16 \pm 0.07 (-13.8%)	0.33 \pm 0.15 (-27.8%)	0.42\pm0.05 (-5.1%)	0.35 \pm 0.07 (-9.3%)	0.34 \pm 0.03 (+1.5%)
PokeCube	0.16 \pm 0.01 (-5.3%)	0.40 \pm 0.05 (-6.9%)	0.41\pm0.02 (+0.1%)	0.36 \pm 0.08 (-6.9%)	0.38 \pm 0.01 (-2.7%)
PullCube	0.33 \pm 0.04 (-10.9%)	0.37 \pm 0.03 (+1.1%)	0.49 \pm 0.05 (+0.3%)	0.50\pm0.12 (+2.3%)	0.50\pm0.08 (-0.8%)
PullCubeTool	0.22 \pm 0.07 (-1.4%)	0.41 \pm 0.24 (-33.8%)	0.60 \pm 0.20 (-4.0%)	0.29 \pm 0.08 (-20.8%)	0.61\pm0.18 (-17.2%)
PushCube	0.26 \pm 0.05 (-11.7%)	0.45 \pm 0.23 (-2.0%)	0.45 \pm 0.06 (-2.6%)	0.45 \pm 0.09 (-3.2%)	0.48\pm0.06 (+6.9%)
PlaceAppleInBowl	0.07 \pm 0.02 (-0.8%)	0.13 \pm 0.02 (-22.5%)	0.11 \pm 0.07 (-7.6%)	0.10 \pm 0.04 (-14.3%)	0.28\pm0.16 (-10.0%)
TransportBox	0.06 \pm 0.04 (+27.8%)	0.24 \pm 0.07 (-6.9%)	0.26 \pm 0.00 (-0.8%)	0.24 \pm 0.09 (-1.3%)	0.28\pm0.01 (-0.3%)

Table 17: Medium Camera Fov Test

Task	SAC AE	DrQ-v2	MaDi	SADA	SegDAC
LiftPegUpright	0.19 \pm 0.00 (-11.7%)	0.19 \pm 0.01 (-59.3%)	0.21 \pm 0.00 (-5.5%)	0.21 \pm 0.01 (-3.6%)	0.22\pm0.00 (-47.6%)
PickCube	0.02 \pm 0.02 (-88.9%)	0.02 \pm 0.01 (-96.7%)	0.08 \pm 0.02 (-82.8%)	0.11\pm0.02 (-71.7%)	0.06 \pm 0.02 (-81.7%)
PokeCube	0.01 \pm 0.01 (-92.3%)	0.02 \pm 0.01 (-95.8%)	0.09 \pm 0.02 (-78.7%)	0.11\pm0.02 (-71.6%)	0.09 \pm 0.01 (-75.8%)
PullCube	0.05 \pm 0.02 (-86.9%)	0.03 \pm 0.02 (-92.8%)	0.15 \pm 0.03 (-69.0%)	0.19\pm0.03 (-60.1%)	0.18 \pm 0.02 (-64.9%)
PullCubeTool	0.02 \pm 0.01 (-90.0%)	0.03 \pm 0.05 (-95.2%)	0.10 \pm 0.02 (-83.2%)	0.15 \pm 0.05 (-58.7%)	0.30\pm0.10 (-59.3%)
PushCube	0.02 \pm 0.02 (-91.7%)	0.02 \pm 0.01 (-96.4%)	0.06 \pm 0.02 (-87.5%)	0.16\pm0.03 (-65.4%)	0.08 \pm 0.03 (-82.6%)
PlaceAppleInBowl	0.01 \pm 0.01 (-80.9%)	0.03\pm0.01 (-82.1%)	0.03\pm0.02 (-77.5%)	0.03\pm0.04 (-71.5%)	0.03\pm0.04 (-89.6%)
TransportBox	0.03 \pm 0.03 (-32.9%)	0.18 \pm 0.07 (-31.8%)	0.20 \pm 0.06 (-21.8%)	0.16 \pm 0.08 (-33.6%)	0.27\pm0.01 (-1.8%)

Table 18: Medium Camera Pose Test

Task	SAC AE	DrQ-v2	MaDi	SADA	SegDAC
LiftPegUpright	0.19±0.01 (-10.9%)	0.19±0.01 (-59.0%)	0.20±0.02 (-10.1%)	0.19±0.01 (-13.3%)	0.23±0.01 (-45.3%)
PickCube	0.03±0.01 (-84.4%)	0.03±0.01 (-94.5%)	0.07±0.02 (-84.8%)	0.11±0.02 (-71.8%)	0.12±0.04 (-64.7%)
PokeCube	0.02±0.02 (-86.4%)	0.02±0.03 (-95.9%)	0.08±0.02 (-79.6%)	0.11±0.02 (-72.8%)	0.10±0.01 (-74.6%)
PullCube	0.04±0.01 (-90.5%)	0.02±0.02 (-95.9%)	0.06±0.03 (-87.5%)	0.16±0.04 (-66.9%)	0.07±0.02 (-85.4%)
PullCubeTool	<u>0.02±0.02 (-91.1%)</u>	0.01±0.01 (-99.1%)	0.01±0.01 (-98.8%)	0.03±0.01 (-93.1%)	0.01±0.01 (-98.4%)
PushCube	0.04±0.01 (-85.6%)	0.02±0.01 (-94.8%)	0.10±0.01 (-78.6%)	0.10±0.03 (-78.8%)	0.34±0.06 (-24.7%)
PlaceAppleInBowl	0.01±0.01 (-86.5%)	0.05±0.03 (-70.6%)	0.03±0.02 (-77.6%)	0.08±0.06 (-34.5%)	0.05±0.08 (-84.3%)
TransportBox	0.04±0.03 (-29.4%)	0.06±0.02 (-75.9%)	0.10±0.06 (-61.8%)	0.14±0.08 (-44.7%)	0.27±0.02 (-3.2%)

Table 19: Medium Ground Color Test

Task	SAC AE	DrQ-v2	MaDi	SADA	SegDAC
LiftPegUpright	0.21±0.00 (-1.1%)	0.21±0.02 (-55.3%)	0.22±0.02 (-0.9%)	0.21±0.04 (-3.0%)	0.39±0.16 (-5.1%)
PickCube	0.04±0.02 (-80.1%)	0.02±0.01 (-96.7%)	0.43±0.06 (-1.5%)	0.35±0.04 (-8.4%)	0.33±0.05 (-2.2%)
PokeCube	0.12±0.05 (-28.7%)	0.09±0.07 (-79.9%)	0.41±0.02 (-0.3%)	0.32±0.08 (-18.0%)	0.38±0.03 (-4.3%)
PullCube	0.18±0.05 (-50.9%)	0.02±0.08 (-95.7%)	0.34±0.14 (-30.1%)	0.33±0.10 (-31.7%)	0.55±0.06 (+10.5%)
PullCubeTool	0.16±0.08 (-25.4%)	0.09±0.12 (-85.4%)	0.47±0.16 (-24.6%)	0.29±0.07 (-20.5%)	0.59±0.12 (-20.8%)
PushCube	0.23±0.02 (-23.4%)	0.03±0.05 (-92.4%)	0.43±0.09 (-7.3%)	0.38±0.11 (-17.0%)	0.47±0.03 (+4.0%)
PlaceAppleInBowl	<u>0.08±0.03 (+1.1%)</u>	0.01±0.04 (-95.9%)	0.10±0.04 (-21.2%)	0.10±0.04 (-15.0%)	0.30±0.16 (-4.4%)
TransportBox	0.04±0.02 (-20.3%)	0.05±0.08 (-81.0%)	0.26±0.01 (-1.1%)	0.23±0.10 (-6.3%)	0.28±0.01 (-0.1%)

Table 20: Medium Ground Texture Test

Task	SAC AE	DrQ-v2	MaDi	SADA	SegDAC
LiftPegUpright	0.21±0.01 (-1.3%)	0.42±0.18 (-10.7%)	0.22±0.01 (-0.1%)	0.22±0.04 (+1.2%)	0.39±0.15 (-4.2%)
PickCube	0.07±0.01 (-59.5%)	0.39±0.03 (-15.8%)	0.43±0.06 (-1.6%)	0.36±0.04 (-6.7%)	0.33±0.03 (-3.1%)
PokeCube	0.13±0.02 (-22.4%)	0.40±0.09 (-7.7%)	0.40±0.01 (-2.2%)	0.25±0.09 (-36.3%)	0.39±0.02 (-1.5%)
PullCube	0.15±0.04 (-58.8%)	0.31±0.02 (-16.0%)	0.26±0.06 (-46.6%)	0.24±0.04 (-50.6%)	0.51±0.06 (+1.6%)
PullCubeTool	0.19±0.04 (-13.7%)	0.56±0.13 (-9.6%)	0.58±0.19 (-7.0%)	0.30±0.15 (-16.8%)	0.72±0.14 (-3.3%)
PushCube	0.14±0.03 (-53.3%)	0.43±0.22 (-6.7%)	0.44±0.08 (-4.4%)	0.33±0.08 (-27.7%)	0.49±0.06 (+9.1%)
PlaceAppleInBowl	0.01±0.01 (-87.4%)	0.00±0.01 (-97.4%)	0.06±0.05 (-47.2%)	0.10±0.04 (-15.8%)	0.30±0.16 (-6.4%)
TransportBox	0.04±0.04 (-26.2%)	0.11±0.10 (-58.6%)	0.11±0.06 (-58.4%)	0.09±0.05 (-62.5%)	0.28±0.01 (-1.1%)

Table 21: Medium Lighting Color Test

Task	SAC AE	DrQ-v2	MaDi	SADA	SegDAC
LiftPegUpright	0.21±0.00 (-2.0%)	0.19±0.00 (-60.2%)	0.22±0.01 (-0.6%)	0.23±0.03 (+2.5%)	0.43±0.16 (+4.3%)
PickCube	0.05±0.01 (-70.7%)	0.01±0.01 (-98.3%)	0.19±0.02 (-56.1%)	0.10±0.05 (-73.0%)	<u>0.16±0.02 (-51.9%)</u>
PokeCube	0.06±0.04 (-60.8%)	0.06±0.05 (-85.8%)	0.38±0.03 (-8.3%)	0.18±0.07 (-53.1%)	0.30±0.03 (-24.1%)
PullCube	0.20±0.06 (-47.0%)	0.05±0.03 (-86.8%)	0.37±0.05 (-24.0%)	0.29±0.11 (-41.4%)	0.49±0.08 (-1.9%)
PullCubeTool	0.12±0.04 (-45.6%)	0.06±0.03 (-90.4%)	0.15±0.12 (-76.3%)	0.32±0.15 (-12.5%)	0.55±0.13 (-26.0%)
PushCube	0.18±0.03 (-39.7%)	0.03±0.03 (-92.9%)	0.48±0.10 (+2.9%)	0.32±0.05 (-31.0%)	0.53±0.06 (+18.1%)
PlaceAppleInBowl	0.05±0.01 (-32.0%)	0.01±0.01 (-91.0%)	0.07±0.04 (-41.7%)	0.10±0.04 (-17.4%)	0.28±0.14 (-11.2%)
TransportBox	0.05±0.03 (+4.9%)	0.26±0.07 (-0.6%)	0.26±0.01 (-0.0%)	0.25±0.09 (+0.4%)	0.28±0.01 (+0.4%)

Table 22: Medium Lighting Direction Test

Task	SAC AE	DrQ-v2	MaDi	SADA	SegDAC
LiftPegUpright	0.21±0.01 (-0.6%)	0.23±0.03 (-51.0%)	0.21±0.01 (-2.4%)	0.22±0.04 (-0.6%)	0.42±0.16 (+1.3%)
PickCube	0.16±0.03 (-14.0%)	0.36±0.10 (-21.2%)	0.43±0.05 (-2.7%)	0.35±0.05 (-8.7%)	0.24±0.04 (-28.2%)
PokeCube	0.15±0.01 (-7.2%)	0.30±0.09 (-30.0%)	0.41±0.02 (-0.3%)	0.36±0.07 (-7.3%)	0.36±0.03 (-7.0%)
PullCube	0.28±0.01 (-24.2%)	0.34±0.10 (-6.8%)	0.49±0.03 (-1.3%)	0.49±0.07 (+1.4%)	0.50±0.07 (+0.5%)
PullCubeTool	0.22±0.06 (+1.4%)	0.47±0.20 (-25.1%)	0.58±0.20 (-6.3%)	0.30±0.10 (-18.7%)	0.71±0.12 (-4.0%)
PushCube	0.25±0.04 (-16.8%)	0.51±0.24 (+12.7%)	0.46±0.10 (-1.1%)	0.46±0.05 (-1.3%)	0.48±0.05 (+6.8%)
PlaceAppleInBowl	0.07±0.02 (+0.3%)	0.14±0.03 (-13.5%)	0.12±0.04 (+0.0%)	0.12±0.04 (+0.8%)	0.29±0.15 (-7.3%)
TransportBox	0.05±0.03 (+0.3%)	0.26±0.07 (-0.4%)	0.26±0.01 (-0.0%)	0.25±0.09 (+0.0%)	0.28±0.01 (+0.2%)

Table 23: Medium Mo Color Test

Task	SAC AE	DrQ-v2	MaDi	SADA	SegDAC
LiftPegUpright	0.20±0.01 (-5.4%)	0.23±0.04 (-51.3%)	0.21±0.01 (-4.8%)	0.22±0.01 (-0.2%)	0.41±0.15 (-0.7%)
PickCube	0.11±0.03 (-37.7%)	0.21±0.12 (-53.3%)	0.02±0.01 (-96.3%)	0.22±0.09 (-43.6%)	0.27±0.05 (-18.8%)
PokeCube	0.07±0.01 (-55.0%)	0.02±0.02 (-96.1%)	0.07±0.15 (-83.2%)	0.17±0.03 (-55.4%)	0.40±0.04 (+1.5%)
PullCube	0.15±0.05 (-60.0%)	0.08±0.02 (-77.8%)	0.10±0.06 (-79.1%)	0.46±0.12 (-5.4%)	0.47±0.07 (-6.4%)
PullCubeTool	0.09±0.02 (-59.0%)	0.03±0.04 (-94.8%)	0.12±0.05 (-80.1%)	0.25±0.17 (-30.6%)	0.49±0.06 (-34.1%)
PushCube	0.15±0.01 (-48.7%)	0.01±0.00 (-96.7%)	0.09±0.03 (-80.1%)	0.41±0.16 (-11.3%)	0.47±0.03 (+4.7%)
PlaceAppleInBowl	0.01±0.00 (-80.0%)	0.01±0.00 (-95.2%)	0.06±0.03 (-52.2%)	0.04±0.04 (-64.2%)	0.29±0.16 (-8.3%)
TransportBox	0.05±0.03 (-1.0%)	0.16±0.10 (-39.0%)	0.26±0.01 (-0.3%)	0.23±0.09 (-5.5%)	0.28±0.01 (+0.3%)

Table 24: Medium Mo Texture Test

Task	SAC AE	DrQ-v2	MaDi	SADA	SegDAC
LiftPegUpright	0.20±0.01 (-5.5%)	0.20±0.00 (-58.6%)	0.20±0.00 (-10.2%)	0.21±0.01 (-5.2%)	0.30±0.09 (-27.5%)
PickCube	0.05±0.02 (-71.1%)	0.01±0.00 (-97.3%)	0.01±0.00 (-98.1%)	0.02±0.02 (-94.3%)	0.10±0.02 (-70.2%)
PokeCube	0.08±0.01 (-52.4%)	0.07±0.02 (-84.4%)	0.16±0.10 (-60.8%)	0.06±0.02 (-85.6%)	0.26±0.05 (-32.4%)
PullCube	0.10±0.01 (-72.0%)	0.08±0.01 (-77.4%)	0.12±0.07 (-76.6%)	0.08±0.04 (-83.1%)	0.47±0.07 (-6.8%)
PullCubeTool	0.07±0.02 (-68.1%)	0.02±0.01 (-96.5%)	0.04±0.03 (-93.0%)	0.04±0.07 (-89.1%)	0.20±0.08 (-73.1%)
PushCube	0.11±0.03 (-62.1%)	0.02±0.00 (-96.5%)	0.10±0.04 (-78.9%)	0.06±0.02 (-86.8%)	0.46±0.05 (+1.9%)
PlaceAppleInBowl	0.03±0.01 (-60.1%)	0.04±0.02 (-78.1%)	0.04±0.02 (-67.8%)	0.03±0.03 (-73.4%)	0.29±0.17 (-6.7%)
TransportBox	0.05±0.04 (+4.1%)	0.25±0.08 (-4.9%)	0.26±0.01 (-0.0%)	0.23±0.09 (-5.4%)	0.28±0.01 (-0.3%)

Table 25: Medium Ro Color Test

Task	SAC AE	DrQ-v2	MaDi	SADA	SegDAC
LiftPegUpright	N/A	N/A	N/A	N/A	N/A
PickCube	N/A	N/A	N/A	N/A	N/A
PokeCube	0.16±0.02 (-5.1%)	0.30±0.06 (-30.2%)	0.41±0.02 (-0.9%)	0.36±0.07 (-8.0%)	0.38±0.03 (-3.0%)
PullCube	0.30±0.05 (-18.4%)	0.16±0.09 (-57.3%)	0.51±0.11 (+3.8%)	0.53±0.19 (+9.2%)	0.50±0.06 (+0.6%)
PullCubeTool	0.21±0.06 (-2.5%)	0.54±0.26 (-12.6%)	0.63±0.20 (+0.6%)	0.33±0.21 (-10.4%)	0.70±0.11 (-5.1%)
PushCube	0.25±0.03 (-14.7%)	0.35±0.23 (-24.3%)	0.49±0.07 (+6.1%)	0.45±0.10 (-2.2%)	0.45±0.05 (+0.4%)
PlaceAppleInBowl	0.08±0.02 (+12.4%)	0.14±0.03 (-17.0%)	0.11±0.05 (-6.7%)	0.12±0.04 (-2.9%)	0.25±0.09 (-19.5%)
TransportBox	N/A	N/A	N/A	N/A	N/A

Table 26: Medium Ro Texture Test

Task	SAC AE	DrQ-v2	MaDi	SADA	SegDAC
LiftPegUpright	N/A	N/A	N/A	N/A	N/A
PickCube	N/A	N/A	N/A	N/A	N/A
PokeCube	0.17±0.02 (+3.2%)	0.32±0.04 (-26.8%)	0.41±0.01 (-1.0%)	0.37±0.08 (-5.1%)	0.39±0.03 (-1.4%)
PullCube	0.35±0.04 (-6.4%)	0.09±0.08 (-75.1%)	0.43±0.09 (-12.3%)	0.60±0.11 (+22.6%)	0.51±0.06 (+2.6%)
PullCubeTool	0.20±0.07 (-9.9%)	0.50±0.23 (-18.8%)	0.67±0.19 (+7.2%)	0.33±0.17 (-10.8%)	0.70±0.14 (-5.9%)
PushCube	0.24±0.04 (-19.3%)	0.28±0.23 (-38.1%)	0.46±0.07 (-1.2%)	0.52±0.08 (+13.6%)	0.50±0.04 (+12.0%)
PlaceAppleInBowl	0.07±0.03 (-1.4%)	0.14±0.03 (-14.0%)	0.12±0.05 (+1.3%)	0.12±0.04 (+0.6%)	0.22±0.12 (-29.0%)
TransportBox	N/A	N/A	N/A	N/A	N/A

Table 27: Medium Table Color Test

Task	SAC AE	DrQ-v2	MaDi	SADA	SegDAC
LiftPegUpright	0.21±0.01 (-3.3%)	0.19±0.00 (-60.0%)	0.20±0.01 (-10.9%)	0.22±0.03 (+0.6%)	0.38±0.13 (-6.7%)
PickCube	0.04±0.00 (-79.6%)	0.00±0.00 (-99.1%)	0.06±0.04 (-85.6%)	0.08±0.02 (-80.0%)	0.17±0.04 (-48.9%)
PokeCube	0.08±0.03 (-53.4%)	0.05±0.05 (-89.3%)	0.23±0.12 (-44.9%)	0.29±0.05 (-25.9%)	0.28±0.02 (-28.4%)
PullCube	0.12±0.09 (-66.4%)	0.03±0.03 (-90.7%)	0.36±0.20 (-27.0%)	0.36±0.06 (-26.2%)	0.42±0.06 (-15.9%)
PullCubeTool	0.12±0.09 (-44.9%)	0.06±0.04 (-90.9%)	0.09±0.02 (-85.6%)	0.19±0.10 (-48.7%)	0.46±0.07 (-37.6%)
PushCube	0.13±0.05 (-56.0%)	0.05±0.03 (-89.5%)	0.12±0.09 (-74.3%)	0.31±0.03 (-33.4%)	0.63±0.12 (+39.3%)
PlaceAppleInBowl	0.02±0.02 (-66.4%)	0.03±0.02 (-81.0%)	0.03±0.02 (-79.0%)	0.09±0.04 (-21.7%)	0.28±0.15 (-11.1%)
TransportBox	0.03±0.04 (-37.4%)	0.04±0.04 (-84.6%)	0.19±0.08 (-27.4%)	0.21±0.09 (-15.7%)	0.28±0.01 (-0.7%)

Table 28: Medium Table Texture Test

Task	SAC AE	DrQ-v2	MaDi	SADA	SegDAC
LiftPegUpright	0.21±0.01 (-2.5%)	0.19±0.00 (-60.2%)	0.22±0.01 (-1.1%)	0.22±0.04 (-2.3%)	0.41±0.15 (-1.3%)
PickCube	0.11±0.04 (-39.8%)	0.02±0.01 (-96.4%)	0.30±0.08 (-30.9%)	0.15±0.05 (-61.2%)	0.23±0.06 (-32.8%)
PokeCube	0.12±0.02 (-25.6%)	0.03±0.02 (-92.2%)	0.37±0.07 (-8.7%)	0.17±0.03 (-55.3%)	0.32±0.04 (-18.8%)
PullCube	0.06±0.03 (-82.4%)	0.01±0.00 (-97.0%)	0.41±0.07 (-17.0%)	0.37±0.08 (-23.4%)	0.49±0.04 (-2.3%)
PullCubeTool	0.06±0.09 (-72.1%)	0.05±0.09 (-92.3%)	0.54±0.19 (-13.4%)	0.09±0.10 (-75.0%)	0.64±0.13 (-13.3%)
PushCube	0.19±0.04 (-36.0%)	0.02±0.02 (-95.3%)	0.40±0.08 (-13.0%)	0.21±0.06 (-54.5%)	0.43±0.07 (-3.6%)
PlaceAppleInBowl	0.01±0.00 (-90.7%)	0.02±0.01 (-90.5%)	0.01±0.02 (-88.8%)	0.04±0.02 (-64.5%)	0.29±0.14 (-8.6%)
TransportBox	<u>0.05±0.03 (+2.9%)</u>	0.14±0.04 (-45.6%)	0.23±0.03 (-13.0%)	0.17±0.10 (-28.8%)	0.28±0.01 (+0.2%)

Table 29: Hard Camera Fov Test

Task	SAC AE	DrQ-v2	MaDi	SADA	SegDAC
LiftPegUpright	0.19±0.00 (-12.7%)	0.19±0.01 (-59.9%)	0.20±0.01 (-10.2%)	0.20±0.02 (-9.5%)	0.20±0.01 (-51.8%)
PickCube	0.02±0.01 (-91.6%)	0.02±0.00 (-95.0%)	0.03±0.03 (-93.0%)	0.06±0.03 (-84.0%)	0.07±0.02 (-78.7%)
PokeCube	0.02±0.02 (-89.9%)	0.02±0.01 (-95.2%)	0.02±0.02 (-94.2%)	0.06±0.03 (-85.1%)	0.05±0.01 (-86.3%)
PullCube	0.06±0.03 (-83.6%)	0.01±0.00 (-96.4%)	0.05±0.02 (-89.7%)	0.09±0.03 (-81.2%)	0.11±0.01 (-77.1%)
PullCubeTool	0.02±0.03 (-92.8%)	0.02±0.03 (-96.3%)	0.05±0.02 (-92.2%)	0.03±0.03 (-91.9%)	0.16±0.04 (-78.6%)
PushCube	0.01±0.01 (-95.6%)	0.02±0.03 (-95.4%)	0.04±0.02 (-91.4%)	0.07±0.02 (-85.2%)	0.12±0.05 (-72.5%)
PlaceAppleInBowl	0.01±0.00 (-90.2%)	0.01±0.01 (-91.0%)	0.02±0.02 (-85.7%)	<u>0.02±0.01 (-81.8%)</u>	0.03±0.01 (-90.8%)
TransportBox	0.03±0.03 (-46.0%)	0.10±0.03 (-62.7%)	0.04±0.01 (-84.6%)	0.11±0.04 (-54.0%)	0.28±0.01 (-0.6%)

Table 30: Hard Camera Pose Test

Task	SAC AE	DrQ-v2	MaDi	SADA	SegDAC
LiftPegUpright	0.19±0.00 (-11.6%)	0.19±0.00 (-59.7%)	0.19±0.00 (-13.4%)	0.20±0.01 (-10.0%)	0.20±0.01 (-52.1%)
PickCube	0.01±0.01 (-92.1%)	0.02±0.01 (-96.7%)	0.03±0.02 (-94.2%)	0.03±0.01 (-93.1%)	0.07±0.01 (-79.4%)
PokeCube	0.01±0.01 (-92.1%)	0.01±0.01 (-97.2%)	0.03±0.02 (-93.1%)	0.06±0.02 (-84.9%)	0.05±0.00 (-87.2%)
PullCube	0.02±0.01 (-94.5%)	0.01±0.01 (-98.3%)	0.02±0.01 (-95.3%)	0.05±0.02 (-88.9%)	0.05±0.04 (-89.1%)
PullCubeTool	0.02±0.03 (-92.3%)	0.01±0.01 (-98.1%)	0.01±0.01 (-97.6%)	0.03±0.02 (-90.9%)	0.09±0.05 (-87.3%)
PushCube	0.04±0.03 (-86.7%)	0.01±0.01 (-97.1%)	0.02±0.02 (-95.2%)	0.02±0.01 (-96.6%)	0.10±0.06 (-78.3%)
PlaceAppleInBowl	0.01±0.00 (-93.1%)	0.01±0.01 (-94.5%)	0.01±0.02 (-90.1%)	0.03±0.04 (-71.0%)	0.03±0.02 (-90.9%)
TransportBox	0.03±0.03 (-42.1%)	0.02±0.03 (-91.0%)	0.03±0.03 (-90.4%)	0.06±0.03 (-74.1%)	0.28±0.01 (-1.1%)

Table 31: Hard Ground Color Test

Task	SAC AE	DrQ-v2	MaDi	SADA	SegDAC
LiftPegUpright	0.20±0.01 (-4.6%)	0.19±0.01 (-59.7%)	0.22±0.01 (+0.4%)	0.21±0.01 (-6.5%)	0.38±0.14 (-8.5%)
PickCube	0.02±0.01 (-89.6%)	0.01±0.01 (-96.8%)	0.38±0.06 (-14.2%)	0.09±0.07 (-75.6%)	0.36±0.03 (+6.0%)
PokeCube	0.08±0.02 (-50.3%)	0.01±0.01 (-97.0%)	0.34±0.12 (-16.7%)	0.10±0.03 (-74.2%)	0.35±0.04 (-10.3%)
PullCube	0.01±0.01 (-96.2%)	0.02±0.03 (-94.1%)	0.23±0.21 (-52.3%)	0.38±0.08 (-21.2%)	0.52±0.08 (+3.2%)
PullCubeTool	0.07±0.04 (-66.3%)	0.06±0.06 (-90.4%)	0.46±0.17 (-25.5%)	0.06±0.06 (-84.0%)	0.60±0.14 (-18.5%)
PushCube	0.08±0.05 (-74.7%)	0.02±0.01 (-96.7%)	0.29±0.13 (-38.4%)	0.34±0.10 (-26.3%)	0.47±0.04 (+5.2%)
PlaceAppleInBowl	0.00±0.00 (-96.1%)	0.00±0.00 (-97.4%)	0.03±0.06 (-76.1%)	0.06±0.03 (-50.9%)	0.30±0.16 (-4.0%)
TransportBox	0.05±0.05 (+4.5%)	0.01±0.02 (-95.3%)	0.26±0.02 (-6.6%)	0.23±0.10 (-8.0%)	0.28±0.01 (-0.4%)

Table 32: Hard Ground Texture Test

Task	SAC AE	DrQ-v2	MaDi	SADA	SegDAC
LiftPegUpright	0.21±0.01 (-0.9%)	0.20±0.01 (-57.0%)	0.22±0.01 (+0.0%)	0.21±0.02 (-4.6%)	0.40±0.15 (-2.1%)
PickCube	0.07±0.02 (-61.4%)	0.10±0.06 (-78.9%)	0.43±0.07 (-3.0%)	0.36±0.05 (-6.8%)	0.32±0.02 (-4.2%)
PokeCube	0.10±0.03 (-40.4%)	0.14±0.10 (-67.0%)	0.40±0.01 (-2.1%)	0.27±0.09 (-30.8%)	0.38±0.04 (-3.3%)
PullCube	0.13±0.04 (-64.5%)	0.14±0.06 (-61.1%)	0.31±0.09 (-37.8%)	0.42±0.16 (-14.8%)	0.55±0.05 (+9.6%)
PullCubeTool	0.09±0.04 (-56.6%)	0.08±0.19 (-86.8%)	0.55±0.19 (-12.1%)	0.23±0.07 (-37.2%)	0.68±0.12 (-8.7%)
PushCube	0.12±0.04 (-59.1%)	0.25±0.21 (-46.1%)	0.47±0.09 (+1.9%)	0.39±0.07 (-15.6%)	0.49±0.07 (+9.4%)
PlaceAppleInBowl	0.01±0.00 (-89.1%)	0.00±0.01 (-97.1%)	0.01±0.02 (-88.9%)	0.01±0.01 (-89.3%)	0.27±0.14 (-14.7%)
TransportBox	0.04±0.03 (-12.7%)	0.10±0.11 (-62.2%)	0.07±0.06 (-71.6%)	0.08±0.05 (-66.1%)	0.27±0.01 (-1.6%)

Table 33: Hard Lighting Color Test

Task	SAC AE	DrQ-v2	MaDi	SADA	SegDAC
LiftPegUpright	<u>0.22</u> \pm 0.01 (+0.6%)	0.20 \pm 0.01 (-58.6%)	0.20 \pm 0.01 (-8.9%)	0.22 \pm 0.04 (-2.2%)	0.39 \pm 0.15 (-4.4%)
PickCube	0.02 \pm 0.01 (-91.2%)	0.01 \pm 0.02 (-98.0%)	0.07 \pm 0.03 (-83.7%)	0.07 \pm 0.02 (-82.5%)	0.15 \pm 0.01 (-55.8%)
PokeCube	0.08 \pm 0.02 (-53.6%)	0.03 \pm 0.01 (-93.2%)	0.21 \pm 0.04 (-49.2%)	0.19 \pm 0.03 (-51.5%)	0.37 \pm 0.05 (-4.8%)
PullCube	0.02 \pm 0.01 (-93.4%)	0.04 \pm 0.04 (-89.0%)	0.42 \pm 0.08 (-14.3%)	0.23 \pm 0.10 (-53.7%)	0.49 \pm 0.09 (-2.1%)
PullCubeTool	0.01 \pm 0.02 (-94.2%)	0.03 \pm 0.02 (-95.6%)	0.08 \pm 0.05 (-87.5%)	0.17 \pm 0.12 (-52.3%)	0.57 \pm 0.15 (-23.3%)
PushCube	0.06 \pm 0.01 (-78.4%)	0.04 \pm 0.02 (-90.4%)	0.36 \pm 0.09 (-21.6%)	0.35 \pm 0.09 (-23.1%)	0.54 \pm 0.05 (+21.0%)
PlaceAppleInBowl	0.01 \pm 0.01 (-89.8%)	0.01 \pm 0.00 (-95.2%)	0.01 \pm 0.02 (-93.0%)	0.07 \pm 0.02 (-43.4%)	0.25 \pm 0.12 (-21.2%)
TransportBox	<u>0.05</u> \pm 0.03 (+2.2%)	0.26 \pm 0.07 (-0.3%)	0.26 \pm 0.01 (+0.1%)	0.25 \pm 0.09 (+0.0%)	0.28 \pm 0.01 (-0.2%)

Table 34: Hard Lighting Direction Test

Task	SAC AE	DrQ-v2	MaDi	SADA	SegDAC
LiftPegUpright	0.21 \pm 0.01 (-1.9%)	0.19 \pm 0.01 (-59.5%)	0.22 \pm 0.01 (+2.3%)	0.22 \pm 0.05 (-0.3%)	0.37 \pm 0.12 (-10.3%)
PickCube	0.10 \pm 0.02 (-44.6%)	0.02 \pm 0.01 (-94.6%)	0.40 \pm 0.08 (-8.9%)	0.35 \pm 0.04 (-10.8%)	0.19 \pm 0.02 (-43.1%)
PokeCube	0.13 \pm 0.01 (-22.5%)	0.07 \pm 0.04 (-84.9%)	0.40 \pm 0.02 (-2.2%)	0.35 \pm 0.07 (-10.0%)	0.20 \pm 0.05 (-49.3%)
PullCube	0.17 \pm 0.04 (-54.5%)	0.05 \pm 0.07 (-87.7%)	0.45 \pm 0.04 (-8.7%)	0.52 \pm 0.19 (+7.1%)	0.47 \pm 0.08 (-5.8%)
PullCubeTool	0.17 \pm 0.04 (-24.2%)	0.04 \pm 0.18 (-92.9%)	0.61 \pm 0.18 (-1.4%)	0.32 \pm 0.09 (-11.5%)	0.64 \pm 0.09 (-13.7%)
PushCube	0.21 \pm 0.02 (-29.7%)	0.05 \pm 0.04 (-89.4%)	0.43 \pm 0.07 (-6.9%)	0.44 \pm 0.03 (-4.3%)	0.44 \pm 0.05 (-2.7%)
PlaceAppleInBowl	<u>0.07</u> \pm 0.02 (-3.1%)	0.01 \pm 0.01 (-91.3%)	0.11 \pm 0.04 (-9.0%)	0.10 \pm 0.04 (-15.9%)	0.24 \pm 0.11 (-25.5%)
TransportBox	<u>0.05</u> \pm 0.03 (+1.3%)	0.26 \pm 0.07 (-0.7%)	0.26 \pm 0.01 (+0.0%)	0.24 \pm 0.09 (-0.5%)	0.28 \pm 0.01 (+0.5%)

Table 35: Hard Mo Color Test

Task	SAC AE	DrQ-v2	MaDi	SADA	SegDAC
LiftPegUpright	0.21 \pm 0.01 (-1.6%)	0.19 \pm 0.00 (-59.4%)	0.20 \pm 0.00 (-8.9%)	0.20 \pm 0.01 (-10.3%)	0.39 \pm 0.12 (-5.6%)
PickCube	0.06 \pm 0.02 (-68.2%)	0.02 \pm 0.01 (-96.6%)	0.01 \pm 0.01 (-98.1%)	0.04 \pm 0.02 (-90.0%)	0.28 \pm 0.03 (-17.2%)
PokeCube	0.08 \pm 0.01 (-53.1%)	0.01 \pm 0.01 (-97.1%)	0.01 \pm 0.00 (-97.2%)	0.02 \pm 0.03 (-96.0%)	0.34 \pm 0.05 (-13.8%)
PullCube	0.10 \pm 0.04 (-73.3%)	0.08 \pm 0.01 (-79.5%)	0.12 \pm 0.04 (-75.8%)	0.09 \pm 0.04 (-81.1%)	0.48 \pm 0.07 (-3.9%)
PullCubeTool	0.04 \pm 0.02 (-80.4%)	0.05 \pm 0.12 (-91.8%)	0.07 \pm 0.04 (-89.0%)	0.19 \pm 0.17 (-46.8%)	0.44 \pm 0.10 (-40.2%)
PushCube	0.10 \pm 0.02 (-65.9%)	0.02 \pm 0.00 (-96.4%)	0.08 \pm 0.03 (-82.7%)	0.06 \pm 0.02 (-88.0%)	0.48 \pm 0.05 (+7.0%)
PlaceAppleInBowl	0.02 \pm 0.01 (-78.6%)	0.01 \pm 0.00 (-92.9%)	0.06 \pm 0.02 (-51.9%)	0.06 \pm 0.03 (-46.2%)	0.30 \pm 0.17 (-6.4%)
TransportBox	<u>0.05</u> \pm 0.03 (+1.8%)	0.18 \pm 0.11 (-30.1%)	0.26 \pm 0.01 (-0.9%)	0.24 \pm 0.10 (-2.2%)	0.28 \pm 0.01 (-0.2%)

Table 36: Hard Mo Texture Test

Task	SAC AE	DrQ-v2	MaDi	SADA	SegDAC
LiftPegUpright	0.20 \pm 0.01 (-5.1%)	0.22 \pm 0.01 (-53.9%)	0.21 \pm 0.01 (-4.4%)	0.22 \pm 0.02 (-1.2%)	0.28 \pm 0.08 (-32.3%)
PickCube	0.06 \pm 0.02 (-69.8%)	0.01 \pm 0.00 (-97.0%)	0.01 \pm 0.00 (-98.1%)	0.02 \pm 0.01 (-94.4%)	0.15 \pm 0.01 (-55.2%)
PokeCube	0.08 \pm 0.01 (-54.2%)	0.03 \pm 0.01 (-92.1%)	0.04 \pm 0.09 (-89.4%)	0.02 \pm 0.02 (-95.1%)	0.22 \pm 0.03 (-45.0%)
PullCube	0.12 \pm 0.04 (-66.5%)	0.10 \pm 0.03 (-71.4%)	0.26 \pm 0.12 (-46.2%)	0.10 \pm 0.04 (-79.0%)	0.43 \pm 0.05 (-14.4%)
PullCubeTool	0.13 \pm 0.04 (-40.8%)	0.12 \pm 0.08 (-81.2%)	0.03 \pm 0.02 (-94.6%)	0.02 \pm 0.05 (-94.0%)	0.45 \pm 0.08 (-38.9%)
PushCube	0.13 \pm 0.02 (-55.9%)	0.02 \pm 0.02 (-94.9%)	0.15 \pm 0.07 (-67.7%)	0.08 \pm 0.03 (-82.7%)	0.45 \pm 0.06 (-0.4%)
PlaceAppleInBowl	0.05 \pm 0.02 (-32.0%)	0.05 \pm 0.03 (-70.3%)	0.06 \pm 0.02 (-54.9%)	0.04 \pm 0.04 (-66.6%)	0.29 \pm 0.18 (-7.4%)
TransportBox	<u>0.05</u> \pm 0.03 (+1.6%)	0.18 \pm 0.07 (-28.9%)	0.26 \pm 0.01 (-0.1%)	0.23 \pm 0.09 (-5.2%)	0.28 \pm 0.01 (-0.1%)

Table 37: Hard Ro Color Test

Task	SAC AE	DrQ-v2	MaDi	SADA	SegDAC
LiftPegUpright	N/A	N/A	N/A	N/A	N/A
PickCube	N/A	N/A	N/A	N/A	N/A
PokeCube	0.11 \pm 0.03 (-34.2%)	0.06 \pm 0.01 (-85.9%)	0.30 \pm 0.07 (-27.9%)	0.20 \pm 0.06 (-49.0%)	0.39 \pm 0.05 (+0.0%)
PullCube	0.04 \pm 0.02 (-88.0%)	0.01 \pm 0.01 (-96.4%)	0.09 \pm 0.12 (-82.1%)	0.09 \pm 0.08 (-81.3%)	0.50 \pm 0.05 (-1.2%)
PullCubeTool	0.14 \pm 0.05 (-35.2%)	0.28 \pm 0.09 (-54.7%)	0.42 \pm 0.16 (-32.3%)	0.23 \pm 0.14 (-38.2%)	0.67 \pm 0.18 (-9.0%)
PushCube	0.06 \pm 0.01 (-78.9%)	0.04 \pm 0.01 (-91.3%)	0.29 \pm 0.13 (-38.2%)	0.04 \pm 0.02 (-90.7%)	0.46 \pm 0.04 (+1.7%)
PlaceAppleInBowl	0.04 \pm 0.02 (-52.6%)	0.01 \pm 0.01 (-92.4%)	0.07 \pm 0.03 (-44.3%)	0.11 \pm 0.04 (-11.0%)	0.27 \pm 0.12 (-15.6%)
TransportBox	N/A	N/A	N/A	N/A	N/A

Table 38: Hard Ro Texture Test

Task	SAC AE	DrQ-v2	MaDi	SADA	SegDAC
LiftPegUpright	N/A	N/A	N/A	N/A	N/A
PickCube	N/A	N/A	N/A	N/A	N/A
PokeCube	0.16±0.02 (-4.3%)	0.25±0.01 (-43.2%)	0.40±0.01 (-3.3%)	0.36±0.08 (-6.8%)	0.30±0.06 (-23.7%)
PullCube	0.29±0.08 (-20.7%)	0.06±0.07 (-84.8%)	0.46±0.12 (-6.3%)	0.54±0.12 (+11.5%)	0.52±0.11 (+3.5%)
PullCubeTool	0.18±0.08 (-17.0%)	0.39±0.18 (-37.5%)	0.61±0.19 (-1.2%)	0.31±0.19 (-16.1%)	0.66±0.16 (-11.1%)
PushCube	0.27±0.05 (-10.7%)	0.11±0.11 (-75.4%)	0.51±0.14 (+9.1%)	0.48±0.10 (+4.3%)	0.44±0.07 (-1.5%)
PlaceAppleInBowl	0.08±0.02 (+2.9%)	0.12±0.05 (-24.3%)	0.10±0.06 (-17.0%)	0.13±0.04 (+5.7%)	0.26±0.10 (-16.9%)
TransportBox	N/A	N/A	N/A	N/A	N/A

Table 39: Hard Table Color Test

Task	SAC AE	DrQ-v2	MaDi	SADA	SegDAC
LiftPegUpright	0.19±0.00 (-11.7%)	0.19±0.01 (-60.0%)	0.19±0.00 (-13.0%)	0.22±0.01 (-0.5%)	0.38±0.14 (-8.1%)
PickCube	0.02±0.01 (-88.5%)	0.00±0.00 (-98.9%)	0.02±0.01 (-95.2%)	0.03±0.01 (-92.2%)	0.11±0.01 (-67.9%)
PokeCube	0.02±0.01 (-90.5%)	0.02±0.01 (-95.7%)	0.03±0.03 (-92.6%)	0.12±0.04 (-68.9%)	0.20±0.03 (-49.9%)
PullCube	0.02±0.02 (-94.0%)	0.02±0.02 (-95.9%)	0.09±0.04 (-81.0%)	0.27±0.04 (-43.9%)	0.35±0.07 (-31.1%)
PullCubeTool	0.03±0.02 (-85.9%)	0.03±0.02 (-95.9%)	0.03±0.03 (-94.9%)	0.02±0.03 (-95.5%)	0.14±0.04 (-80.9%)
PushCube	0.04±0.03 (-87.0%)	0.04±0.03 (-91.0%)	0.06±0.03 (-86.3%)	0.17±0.08 (-64.1%)	0.60±0.15 (+33.3%)
PlaceAppleInBowl	0.00±0.01 (-93.4%)	0.01±0.01 (-92.7%)	0.01±0.02 (-95.5%)	0.04±0.05 (-67.5%)	0.25±0.09 (-21.2%)
TransportBox	0.07±0.05 (+45.2%)	0.07±0.10 (-73.6%)	0.12±0.06 (-55.8%)	0.19±0.10 (-20.7%)	0.28±0.01 (-0.6%)

Table 40: Hard Table Texture Test

Task	SAC AE	DrQ-v2	MaDi	SADA	SegDAC
LiftPegUpright	0.19±0.01 (-10.9%)	0.20±0.01 (-58.3%)	0.20±0.01 (-11.2%)	0.20±0.01 (-8.7%)	0.20±0.01 (-51.7%)
PickCube	0.03±0.01 (-83.7%)	0.02±0.01 (-96.0%)	0.05±0.04 (-89.4%)	0.07±0.03 (-82.5%)	0.07±0.02 (-79.9%)
PokeCube	0.07±0.05 (-54.9%)	0.02±0.00 (-96.0%)	0.06±0.03 (-85.4%)	0.08±0.02 (-78.2%)	0.15±0.04 (-62.3%)
PullCube	0.03±0.02 (-93.0%)	0.01±0.00 (-98.4%)	0.12±0.04 (-75.2%)	0.16±0.04 (-67.7%)	0.04±0.03 (-92.5%)
PullCubeTool	0.07±0.07 (-67.7%)	0.03±0.03 (-94.6%)	0.29±0.17 (-53.0%)	0.05±0.03 (-86.5%)	0.02±0.02 (-97.4%)
PushCube	0.04±0.01 (-86.2%)	0.03±0.02 (-92.4%)	0.05±0.03 (-90.2%)	0.08±0.02 (-83.7%)	0.10±0.06 (-78.2%)
PlaceAppleInBowl	0.01±0.00 (-82.9%)	0.01±0.02 (-91.9%)	0.01±0.02 (-91.3%)	0.05±0.02 (-56.9%)	0.25±0.11 (-20.2%)
TransportBox	0.05±0.04 (+7.6%)	0.15±0.08 (-41.3%)	0.24±0.04 (-9.3%)	0.25±0.08 (+3.7%)	0.27±0.01 (-2.2%)

B ABLATIONS

B.1 TEXT INPUTS ABLATION

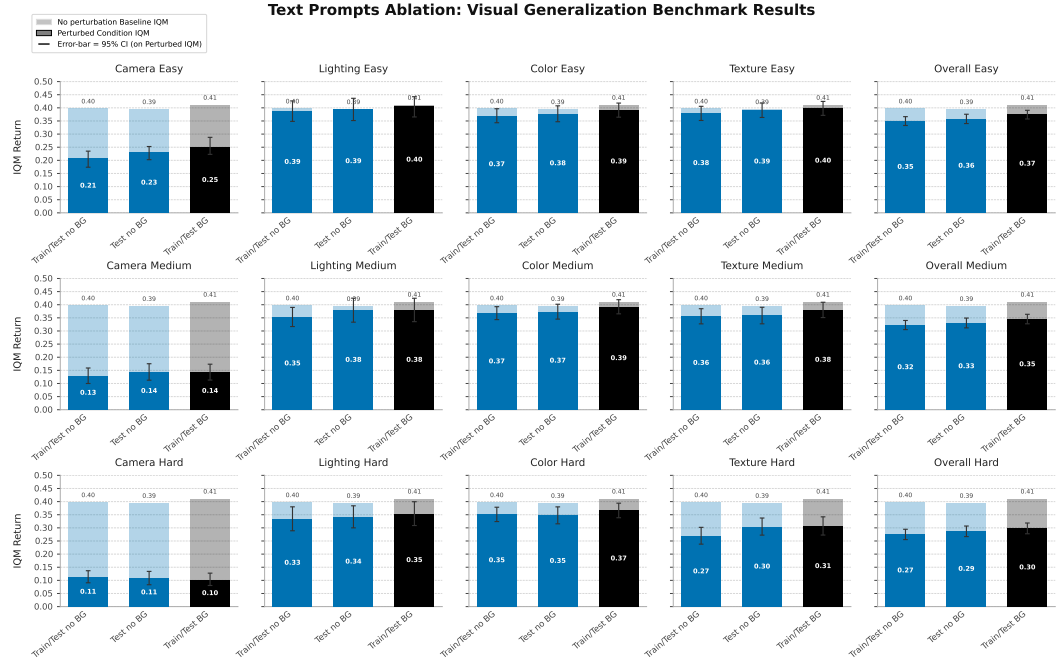


Figure 25: Visual generalization results for the different text tags ablations.

We conducted an ablation to evaluate whether including the "background" text tag improves visual generalization in SegDAC. In the "Train/Test no BG" setting (Figure 25), the model is trained and tested without the "background" tag. For example, in the Push Cube task, the input tags would be ["robot", "gripper", "small box", "target"] instead of ["background", "robot", "gripper", "small box", "target"]. In the "Test no BG" setting, the model is trained with the background tag but tested without it. The final configuration, shown in black in Figure 25, uses the background tag during both training and testing and corresponds to the final version of SegDAC.

The goal of this ablation is to determine whether training with background segments encourages the model to ignore irrelevant information more effectively, or if excluding them allows it to focus more directly on task-relevant objects. While YOLO-World and SAM can still introduce irrelevant segments even without the background tag, our experiments show that including the tag leads to a noticeably larger number of irrelevant segments.

Results in Figure 25 show that all configurations perform similarly, but "Train/Test BG" achieves about $\sim 9\%$ higher IQM returns. This suggests that including the background tag improves generalization by encouraging the model to focus less on distractions.

B.2 OBJECT-CENTRIC VS GLOBAL IMAGE REPRESENTATIONS

To assess whether object-centric representations are more effective than global image features, we compared SegDAC to an SAC baseline that uses a fixed-length global image representation. This baseline, referred to as SAC SAM Encoder, computes the mean of SAM's patch embeddings over the entire image, without using segmentation. The resulting vector is then processed by an MLP with the same number of layers as the projection head used in SegDAC to predict actions or Q-values.

Figure 26 shows the results. SegDAC outperforms SAC SAM Encoder on 7 out of 8 tasks and ties on the remaining one. This highlights a key limitation of directly using pre-trained encoders like SAM for global image representations in online visual RL. Even after attempting hyperparameter tuning for SAC SAM Encoder, we observed no improvement in performance.

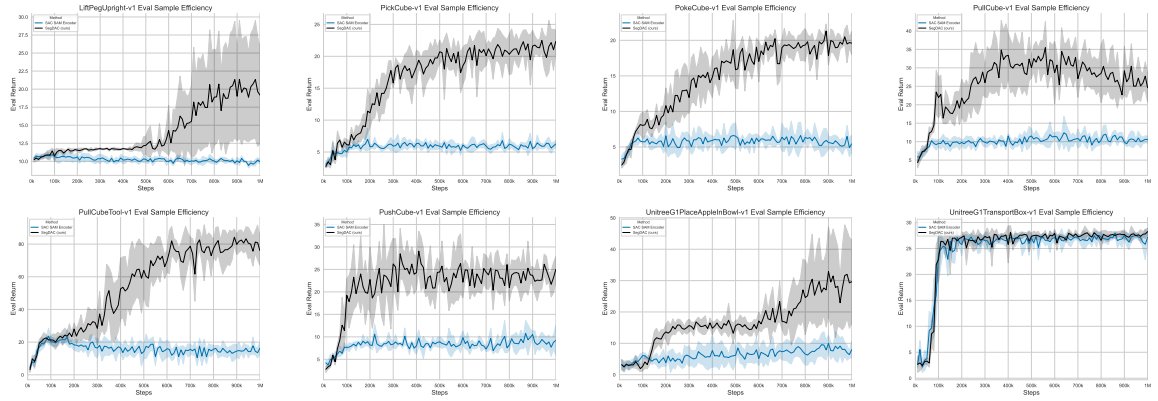


Figure 26: Sample efficiency comparison of SegDAC vs SAC SAM Encoder which uses a global image representation instead of the object-centric representations used by SegDAC.

C TASKS DEFINITIONS

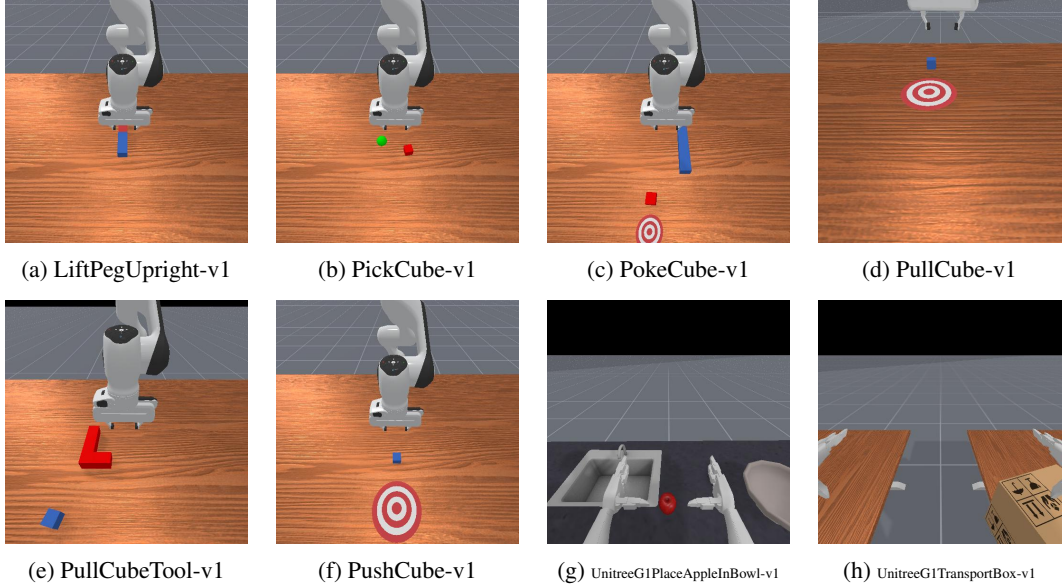


Figure 27: Default (no perturbation) scenes for each of the 8 tasks used for training.

To train SegDAC and the baselines, we used 8 tasks from ManiSkill3 (version `mani_skill==3.0.0b21`) with the default normalized dense reward. The tasks and their corresponding configurations are summarized in table 41 and visualized in figure 27.

Task Name	Max Episode Length	Control Mode
LiftPegUpright-v1	50	PD EE Delta Pos
PickCube-v1*	50	PD EE Delta Pos
PokeCube-v1	50	PD EE Delta Pos
PullCube-v1	50	PD EE Delta Pos
PullCubeTool-v1	100	PD EE Delta Pos
PushCube-v1	50	PD EE Delta Pos
UnitreeG1PlaceAppleInBowl-v1	100	PD Joint Delta Pos
UnitreeG1TransportBox-v1	100	PD Joint Delta Pos

Table 41: Task configurations used for training SegDAC and baselines.

* For the PickCube-v1 task, we created a modified version that makes the visual target sphere visible. This allows vision-based policies to leverage goal information. We achieved this by commenting out the following line in the original task code:

```
# self._hidden_objects.append(self.goal_site)
```

D HYPERPARAMETERS

Each method was trained using its own hyperparameter configuration. Once a configuration was found to perform well for a given method, it was kept fixed across all tasks. For the baselines, we used the official implementations provided by the authors and used their default hyperparameters as starting points. In most cases, these settings were appropriate without modification. The only adjustment we made was to the discount factor, which we set to 0.80 for all methods, as we found this value worked better with ManiSkill3 and is also used in the framework’s official baselines.

For SegDAC, text tags were provided manually per task by a human. However, automatic tagging is also feasible using a VLM or image text tagging models such as RAM++ (Zhang et al., 2023b). We opted for manual tags to reduce the scope of this research and to reduce computational overhead. We did not perform extensive tuning of the tags, instead, we selected simple text tags that seemed to make sense given a static frame and verified that SAM produced reasonable segmentations for them. While more exploration is needed to determine the optimal tags, we found that basic tags performed well in practice.

Note that due to computational constraints, we did not perform an extensive hyperparameter search for SegDAC, and we did not tune the parameters of YOLO-World or SAM.

Tables 43 and 44 summarize the key hyperparameters used for SegDAC and the baselines. We report only the most relevant parameters for reproducibility, omitting architectural defaults that are standard for each algorithm. For the complete list of hyperparameters, readers are invited to check the official code repository on the project page (anonymized for review).

Table 42: Text tags used by SegDAC for each task.

Task	Text Tags
LiftPegUpright-v1	background, robot, gripper, rectangle bar, wooden peg
PickCube-v1	background, robot, gripper, small box, sphere
PushCube-v1	background, robot, gripper, small box, target
PullCube-v1	background, robot, gripper, small box, target
PokeCube-v1	background, robot, gripper, small box, bar, target
PullCubeTool-v1	background, robot, gripper, small box, block
UnitreeG1PlaceAppleInBowl-v1	background, robot, robot hand, gripper, apple, bowl
UnitreeG1TransportBox-v1	background, robot, robot hand, gripper, box

The list of text tags used by SegDAC for each task is provided in Table 42.

Hyperparameter	SegDAC
Actor learning rate	3×10^{-4}
Critic learning rate	5×10^{-4}
Entropy learning rate	3×10^{-4}
Optimizer	Adam
Gamma (discount)	0.80
Target update rate (τ)	0.01
Actor update frequency	1
Critic update frequency	1
Target networks update frequency	2
Image resolution	512
Min log std	-10
Max log std	2
Embedding dim	128
Transformer decoder layers	6
Transformer decoder heads	8
Transformer decoder hidden size	1024
Transformer dropout	0.0
Projection head	ResidualMLP
Projection head hidden layers	4
Projection head hidden size	256
Projection head norm	LayerNorm
Projection head pre-normalize input	true
Projection head activation	ReLU
YOLO-World	yolov8s-worldv2
YOLO-World Confidence Threshold	0.0001
YOLO-World IoU Threshold	0.01
EfficientViT SAM	efficientvit-sam-l0
Mask post-processing kernel size	9
Segment Embedding Min Pixel	4
Replay Buffer Max Size	1,000,000

Table 43: Key hyperparameters used for training SegDAC.

Note that in SegDAC, the actor and critic each use their own transformer decoder and projection head, but they share the same architecture and hyperparameters. For clarity, we omit separate entries for each and report the shared configuration.

Hyperparameter	SADA	MaDi	DrQ-v2	SAC-AE	SAC State
Actor learning rate	5×10^{-4}	1×10^{-3}	1×10^{-4}	1×10^{-4}	3×10^{-4}
Critic learning rate	5×10^{-4}	1×10^{-3}	1×10^{-4}	1×10^{-3}	3×10^{-3}
Entropy learning rate	5×10^{-4}	1×10^{-4}	—	1×10^{-4}	3×10^{-4}
Target update rate (τ)	0.01	0.01	0.01	0.01	0.01
Actor update frequency	2	2	2	1	1
Critic update frequency	2	1	2	1	1
Target networks update frequency	2	2	2	2	2
Replay buffer size	1,000,000	1,000,000	1,000,000	1,000,000	1,000,000
Gamma (discount)	0.80	0.80	0.80	0.80	0.80
Image resolution	84	84	84	84	—
MLP Projection layers	4	3	4	3	4
MLP Projection dim	1024	1024	1024	1024	256
Frame Stack	3	3	3	3	3
N-step return	—	—	3	—	—
Optimizer	Adam	Adam	Adam	Adam	Adam

Table 44: Key hyperparameters for baseline methods. SAC State uses privileged full state information instead of images.

E SEGMENTATION DETAILS

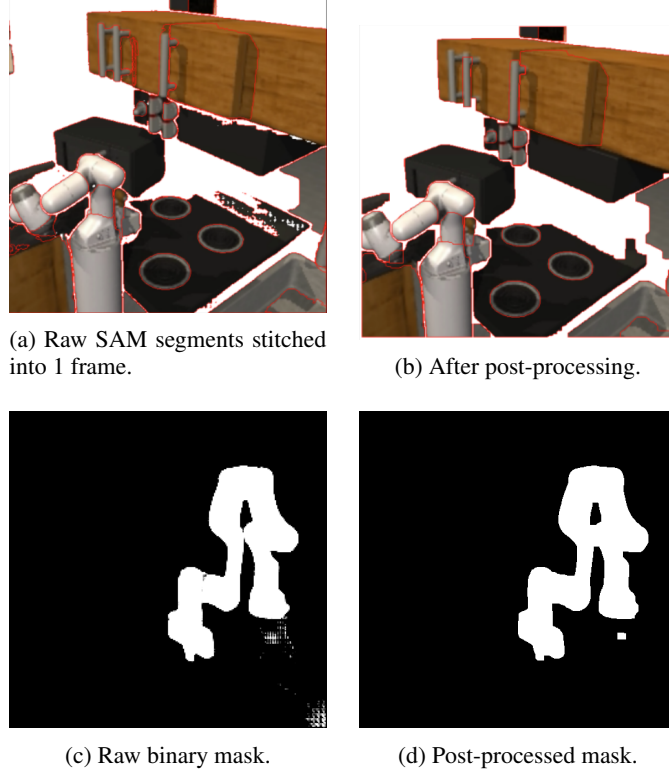


Figure 28: Effect of our lightweight post-processing on SAM outputs. Top: stitched overlays. Bottom: single mask.

To improve the quality of segments predicted by SAM, prior work such as SAM (Kirillov et al., 2023), SAM-G (Wang et al., 2023), and PerSAM (Zhang et al., 2023a) typically rely on heavy post-processing pipelines, often involving iterative mask refinement. In contrast, we adopt a lightweight and efficient approach based on morphological opening and closing operations (Sreedhar, 2012). These classical image processing techniques are fast and effective at removing small artifacts such as holes or sprinkles commonly found in raw segmentation masks. The impact of this post-processing is illustrated in Figure 28.

Our implementation of this post-processing procedure is written in pure PyTorch, as shown below:

```

import torch
import torch.nn.functional as F

...
def post_process_masks(self, masks: torch.Tensor, kernel_size: int)
    """
    masks: (N, 1, H, W)
    """
    opened = self.apply_morphological_opening(
        masks.to(torch.float32), kernel_size=kernel_size
    )
    return self.apply_morphological_closing(opened,
        kernel_size=kernel_size).to(
        torch.uint8
    )

def apply_morphological_opening(

```

```

        self, masks: torch.Tensor, kernel_size: int
    ) -> torch.Tensor:
        eroded = self.apply_erosion(masks, kernel_size)
        return self.apply_dilation(eroded, kernel_size)

def apply_erosion(self, masks: torch.Tensor, kernel_size: int) ->
    torch.Tensor:
    return -self.max_pool2d_same_dim(-masks, kernel_size=kernel_size)

def apply_dilation(self, masks: torch.Tensor, kernel_size: int) ->
    torch.Tensor:
    return self.max_pool2d_same_dim(masks, kernel_size=kernel_size)

def max_pool2d_same_dim(self, masks: torch.Tensor, kernel_size: int):
    stride = 1
    dilation = 1
    pad_h_top, pad_h_bottom = self.compute_padding(
        kernel_size, stride, dilation)
    pad_w_left, pad_w_right = self.compute_padding(
        kernel_size, stride, dilation)

    padded_input = F.pad(
        masks, (pad_w_left, pad_w_right, pad_h_top, pad_h_bottom))

    return F.max_pool2d(
        padded_input, kernel_size=kernel_size, stride=stride,
        dilation=dilation
    )

def compute_padding(self, kernel_size, stride=1, dilation=1):
    padding_total = max(0, (kernel_size - 1) * dilation - stride + 1)
    pad_before = padding_total // 2
    pad_after = padding_total - pad_before
    return pad_before, pad_after

def apply_morphological_closing(
    self, masks: torch.Tensor, kernel_size: int
) -> torch.Tensor:
    dilated = self.apply_dilation(masks, kernel_size)
    return self.apply_erosion(dilated, kernel_size)

```

F SEGMENT EMBEDDINGS EXTRACTION DETAILS

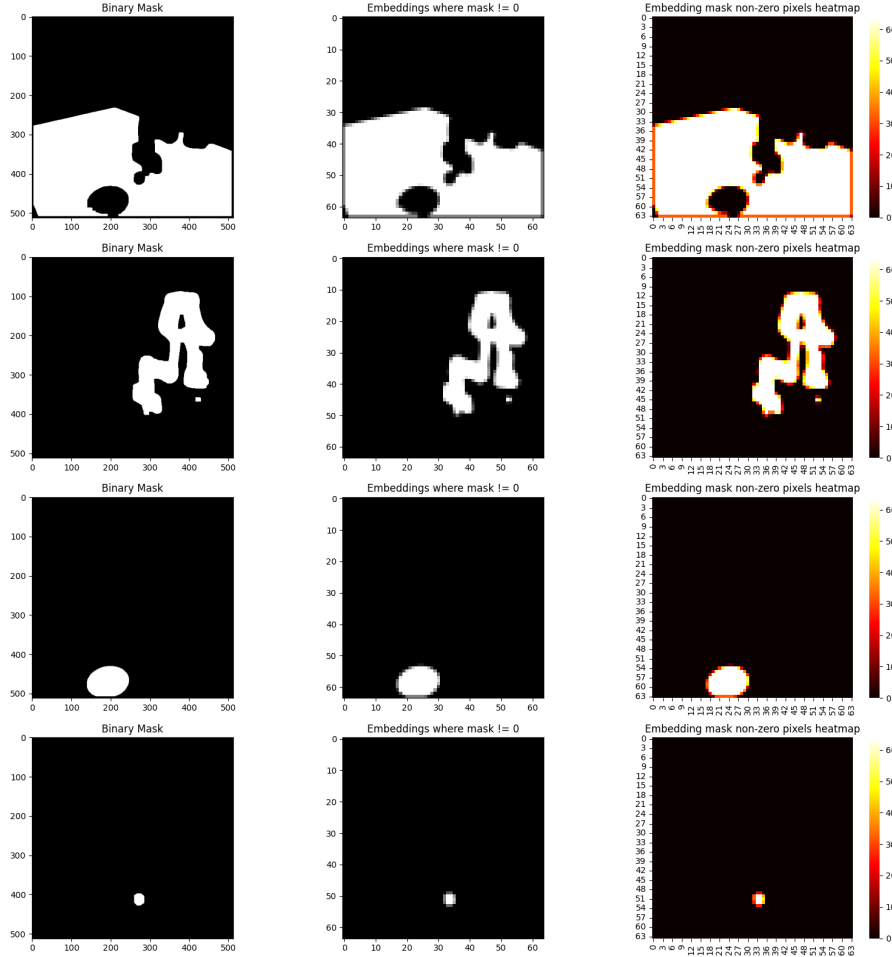


Figure 29: Left: binary mask for the selected segment. Middle: SAM encoder patch grid, showing only patches whose spatial footprint overlaps the mask. Right: per-patch mask–overlap heatmap, defined as the number (or fraction) of mask pixels inside each patch. Boundary patches have lower overlap (red) because they straddle multiple segments, while interior patches approach full coverage (white). This heatmap reflects spatial overlap only, not the contextual information carried by the patch embeddings.

Figure 29 illustrates the relationship between the binary masks produced by our grounded segmentation module (left), the corresponding **overlapping** patch embeddings (middle), and a heatmap showing the pixel count per patch (right). Most patch embeddings have a high pixel count, while those near the mask edges tend to overlap less exclusively with the segment.

G SEGMENT ATTENTION ANALYSIS

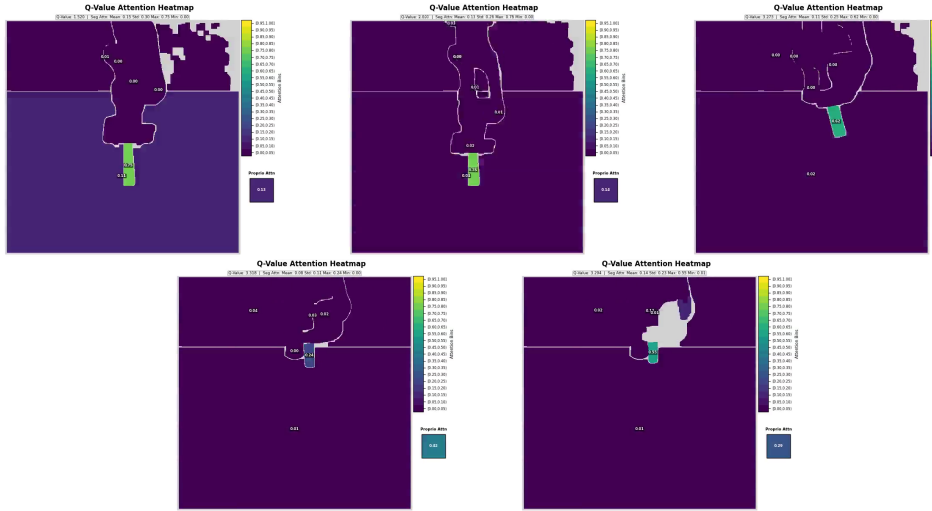


Figure 30: Average segment attention from the critic when predicting Q-values in the LiftPegUpright-v1 task. The trajectory begins in the top-left frame. Grey regions indicate areas where SAM did not detect any segments.

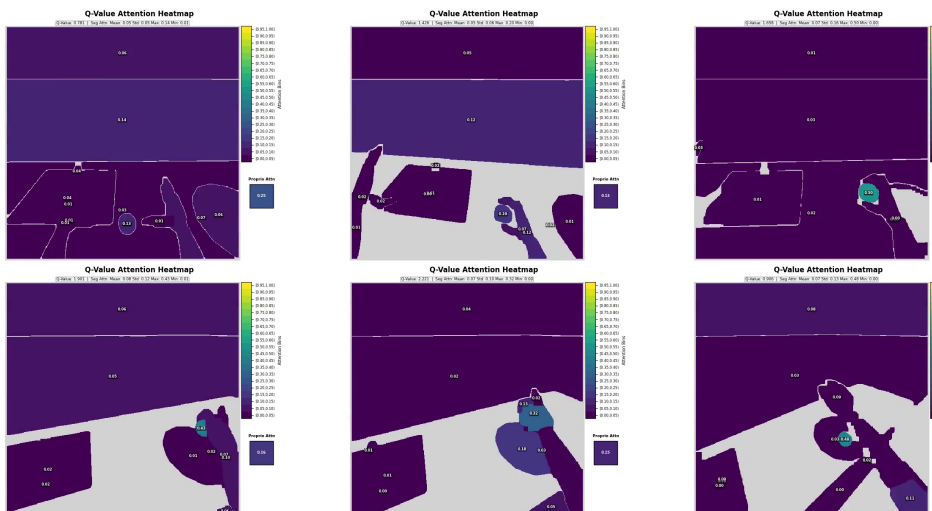


Figure 31: Average segment attention from the critic when predicting Q-values in the UnitreeG1PlaceAppleInBowl-v1 task. The trajectory begins in the top-left frame. Grey regions indicate areas where SAM did not detect any segments.

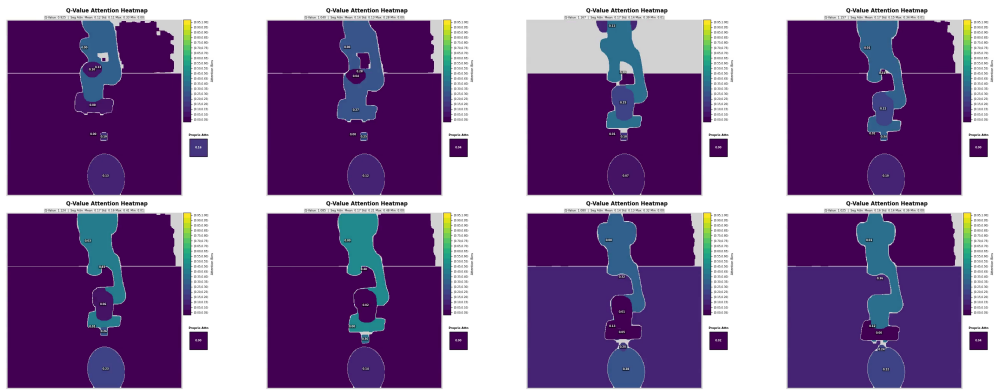


Figure 32: Average segment attention from the critic when predicting Q-values in the PushCube-v1 task. The trajectory begins in the top-left frame. Grey regions indicate areas where SAM did not detect any segments.

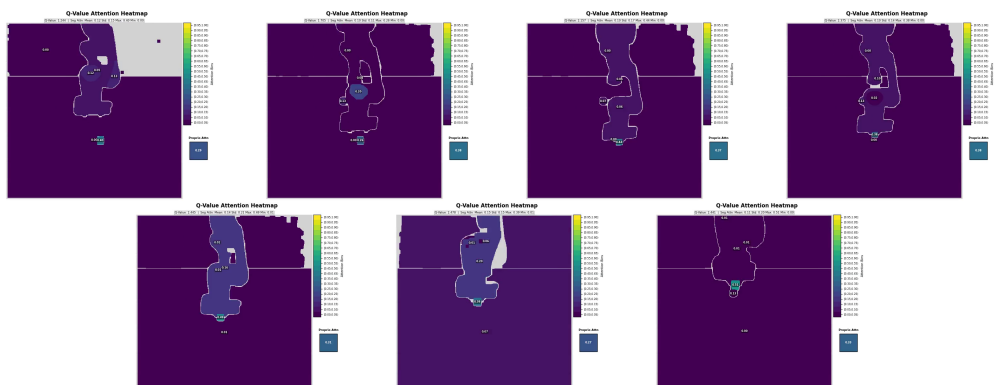


Figure 33: Average segment attention from the critic when predicting Q-values in the PickCube-v1 task. The trajectory begins in the top-left frame. Grey regions indicate areas where SAM did not detect any segments.

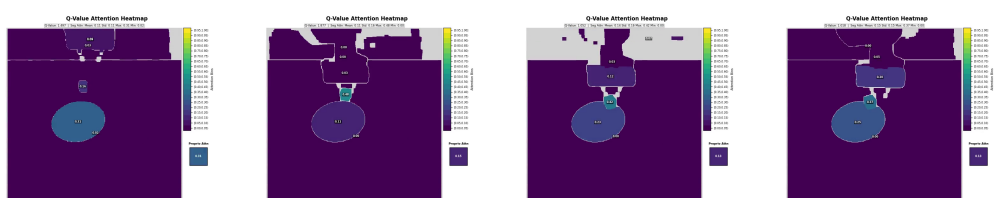


Figure 34: Average segment attention from the critic when predicting Q-values in the PullCube-v1 task. The trajectory begins on the left frame. Grey regions indicate areas where SAM did not detect any segments.

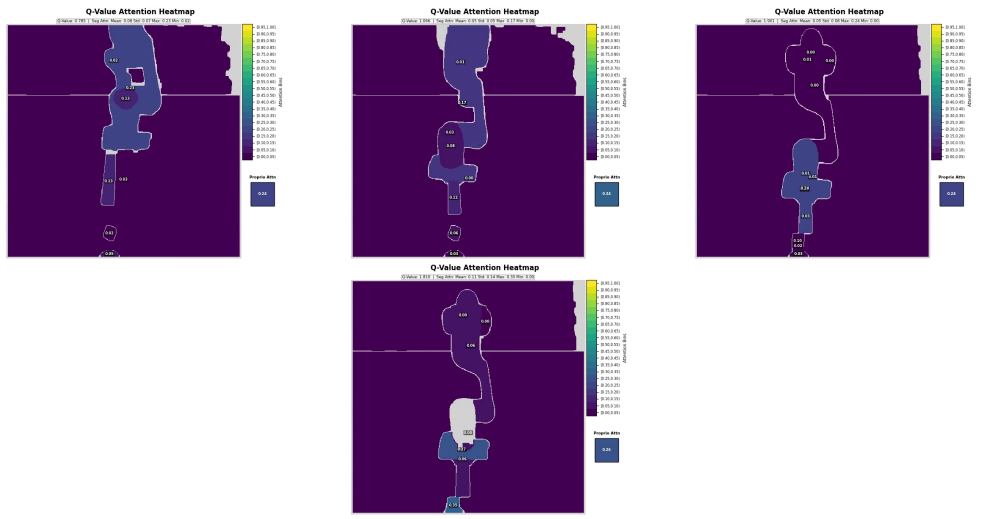


Figure 35: Average segment attention from the critic when predicting Q-values in the PokeCube-v1 task. The trajectory begins in the top-left frame. Grey regions indicate areas where SAM did not detect any segments.

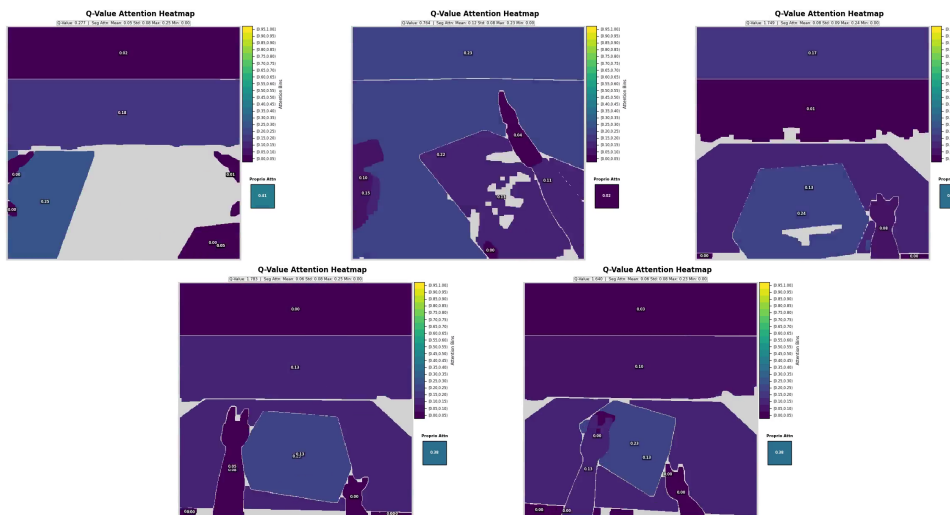


Figure 36: Average segment attention from the critic when predicting Q-values in the UnitreeG1TransportBox-v1 task. The trajectory begins in the top-left frame. Grey regions indicate areas where SAM did not detect any segments.

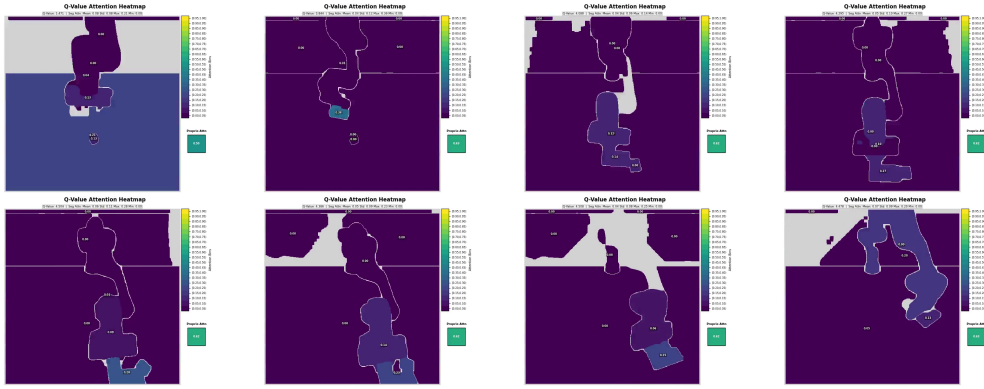


Figure 37: Average segment attention from the critic when predicting Q-values in the PullCubeTool-v1 task. The trajectory begins in the top-left frame. Grey regions indicate areas where SAM did not detect any segments.

Figures 30 to 37 show the average segment attention from the critic when predicting Q-values for all eight tasks. Grey regions indicate areas where SAM did not detect any segments.

We observe that SegDAC consistently attends to task-relevant segments, such as the peg in LiftPegUpright-v1, while ignoring background elements when they provide no useful information. For example, in LiftPegUpright-v1, the peg receives approximately 75% of the attention early in the trajectory. Once the peg is upright, the model shifts some attention to proprioceptive inputs, possibly to stabilize the peg.

SegDAC also demonstrates robustness to variability in detected segments. In PickCube-v1, early frames show the servo button segmented as a small circular region, which the critic uses to guide positioning. In later frames, when the full robot arm is detected instead, the critic adapts and reallocates attention accordingly to complete the task.

Across tasks, SegDAC often allocates significant attention to the manipulation object. For instance, the apple receives about 50% of the attention in UnitreeG1PlaceAppleInBowl-v1. Similarly, in LiftPegUpright-v1, the peg receives around 75% early on.

Figure 33 illustrates that SegDAC is robust to partial occlusions. At the beginning of the trajectory, the goal region is fully occluded by the robot arm, and the model focuses its attention on the cube, which aligns with the sub-goal of grasping it first. As the cube is picked up and the arm moves, the goal region becomes partially visible. Even when it becomes occluded again during the motion, SegDAC continues moving the arm toward the correct location. The goal region becomes visible near the end, and the model successfully completes the task. This shows that SegDAC can handle some level of dynamic occlusions and maintain task-relevant behavior throughout.

H IMPLEMENTATION DETAILS

H.1 POLICY EVALUATION AND DATA COLLECTION

In this work, we use **evaluation** to refer to the policy’s performance under the *no-perturbation* setting during training, which we use to track sample efficiency, samples used for evaluation are not seen during training. **Testing** refers to performance on the *visual generalization benchmark*, which includes various visual perturbations. This distinction separates standard in-distribution evaluation from robustness testing under distribution shifts.

During both evaluation and testing, stochastic policies were run in deterministic mode by taking the mean of their action distributions. We followed the ManiSkill3 evaluation protocol¹, which disables

¹https://maniskill.readthedocs.io/en/v3.0.0b21/user_guide/reinforcement_learning/setup.html#evaluation

early termination to ensure all trajectories have the same length. This makes performance metrics more comparable.

Evaluation metrics were averaged over 5 random seeds, each with 10 rollouts. Proper seeding was applied at the start of both training and evaluation scripts. We used 10 parallel environments to collect evaluation rollouts during training.

For training, we used 20 parallel GPU environments and performed 5 gradient updates per environment step with a batch size of 128, resulting in an update-to-data ratio of 0.25.

H.2 ONLINE RL OPTIMIZATION

Training online RL agents with large models such as SAM on high-resolution images (512x512) is computationally expensive. To complete experiments within one day on a single L40s GPU, we applied various key optimizations.

Prompt-Based Segmentation FTD relied on prompt-free segmentation, which we found to be significantly slower. In our tests, using bounding boxes as prompts for SAM yielded about a 10 \times speedup compared to prompt-free mode. Prompt-based segmentation also provides semantic grounding, making it both faster and better aligned with our design.

Segmentation Post-Processing SAM-G applied iterative refinement, repeatedly invoking SAM to improve mask quality. While effective, this was too slow for online RL. We instead use a lightweight post-processing step that runs in about 1 ms on an L40s GPU. Further details are given in Section E.

Efficient Vision Backbone. We replaced the original SAM model (Kirillov et al., 2023) with EfficientViT-SAM (Zhang et al., 2024), which offers comparable segmentation quality but significantly faster inference speed, approximately 48 \times faster according to the authors. We also tested SAM 2 (Ravi et al., 2024), which improves encoder efficiency but remained significantly slower than EfficientViT-SAM in practice.

All RGB images were processed at a resolution of (3, 512, 512) in (C, H, W) format. This is significantly higher than standard visual RL settings, which often operate in the (3, 84, 84) to (3, 128, 128) range (Laskin et al., 2020; Kostrikov et al., 2021; Srinivas et al., 2020; Hansen & Wang, 2021; Yarats et al., 2021; Bertoin et al., 2023; Almuzairee et al., 2024; Grooten et al., 2023). We used the smallest checkpoint (efficientvit_sam_l0), which natively supports 512 \times 512 images. Reducing the resolution further led to noticeable performance degradation with only marginal speedup, so we retained the native resolution.

We extended EfficientViT-SAM to support batched image embedding computation. This significantly improved throughput since image embedding is the most computationally expensive step. Most SAM variants, including the official implementations, do not support batching. Additionally, we tested prompt-free segmentation but found it to be too slow for our pipeline (10-100x slower), so we opted for guided segmentation using text inputs.

Efficient Network Computation. To optimize network computation, we used `torch.vmap` (Paszke et al., 2019) to batch forward passes across multiple networks, such as the twin critics in SAC. This allowed us to compute their outputs in a single pass, improving efficiency.

Replay Buffer Design. We implemented a custom replay buffer using `TensorDict` (Bou et al., 2023) to efficiently handle the variable number of segments per frame. Since the segment embedding extraction module has no trainable weights, we compute embeddings once during data collection and store them directly in the buffer rather than storing raw images.

This approach reduces both memory usage and compute load. Segment embeddings have dimension 128 \sim 256, and a typical frame has between 4 and 25 segments, this is significantly smaller than the original (3 \times 512 \times 512) image. This also avoids running SAM during training, which would otherwise make online RL infeasible.

Variable-Length Sequence Handling. Since each environment step yields a variable number of segments, a batch of B steps results in a total of N_{total} segments. Padding each sequence to a fixed length would be inefficient and would require an additional per-task hyperparameter. To avoid this, we adopt sequence packing, inspired by recent techniques in large language models (Krell et al., 2022). All segment embeddings are concatenated into a single sequence of shape $(1, N_{\text{total}}, D)$, and a causal attention mask is applied to ensure that each segment only attends to other segments from the same time step. This enables efficient and correct attention computation without the overhead of padding. SegDAC is only limited by available memory for the maximum number of segments it can process.

I PRIOR WORKS COMPARISON

Table 45: Pixel-based RL baselines vs SegDAC.

Criterion	SAC-AE	DrQ-v2	MaDi	SADA	SegDAC (ours)
Needs Human Labels	✓ No	✓ No	✓ No	✓ No	✓ No
Leverages Pretrained Vision Models	✗ No	✗ No	✗ No	✗ No	✓ Yes
Leverages Text	✗ No	✗ No	✗ No	✗ No	✓ Yes
Object-centric representations	✗ No	✗ No	✗ No	✗ No	✓ Yes
Learns In Latent Space	✗ No	✗ No	✗ No	✗ No	✓ Yes
Needs Auxiliary Losses	✗ Yes	✓ No	✓ No	✓ No	✓ No
Needs Data Augs (RL training)	✓ No	✗ Yes	✗ Yes	✗ Yes	✓ No

J SAMPLE EFFICIENCY

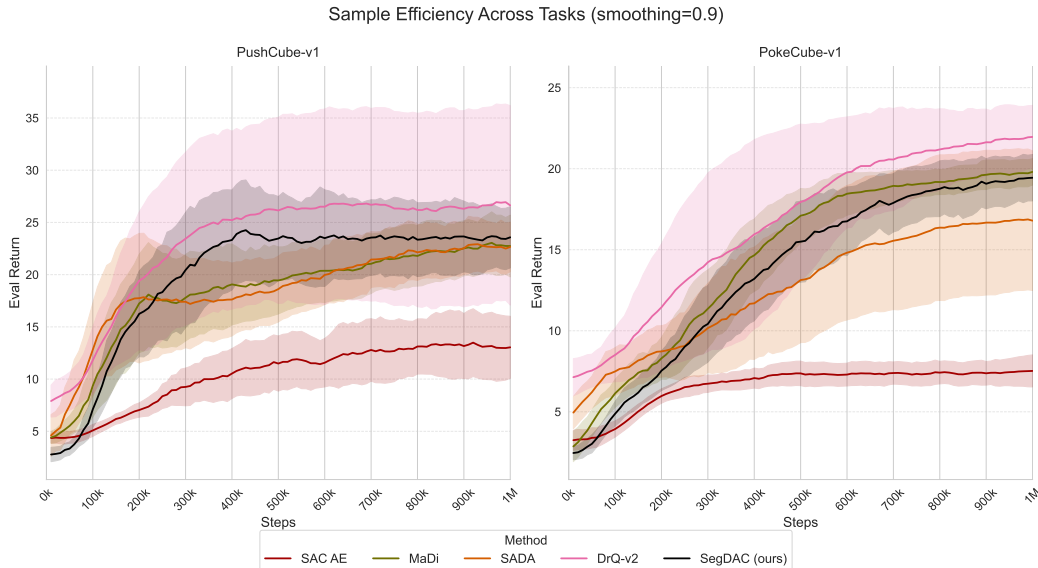


Figure 38: Evaluation return sample efficiency curves for the push/poke cube manipulation tasks.